AD-A040 711 TELEDYNE RYAN AERONAUTICAL CO SAN DIEGO CALIF F/G 17/7
EXPLORATORY DEVELOPMENT OF ADVANCED MISSILE SEEKER TECHNOLOGY.(U)
APR 76 N00024-75-C-5316
UNCLASSIFIED TRA-72469-6 NL

1 OF 1
AD A040711

END
DATE FILMED
7-77

TELEDYNE RYAN ELECTRONICS

Report No. TRA72469-6

B.S.

EXPLORATORY DEVELOPMENT OF ADVANCED MISSILE SEEKER TECHNOLOGY

Teledyne Ryan Aeronautical Co.
2701 Harbor Drive
San Diego, California 92112

25 April 1976

Final Report for Period 1 August 1975 - 19 April 1976

Prepared for:

DEPARTMENT OF THE NAVY
Naval Sea Systems Command
Washington, D.C. 20360

Unclassified

SECURITY CLASSIFICATION OF THIS PAGE (When Data Entered)

REPORT DOCUMENTATION PAGE

READ INSTRUCTIONS BEFORE COMPLETING FORM

1. REPORT NUMBER (14) TR-72469-6	2. GOVT ACCESSION NO. (9)
3. RECIPIENT'S CATALOG NUMBER	
4. TITLE (and Subtitle) (6) Exploratory Development of Advanced Missile Seeker Technology.	5. TYPE OF REPORT & PERIOD COVERED Final Report for Period of 1 August 1975 - 19 April 1976
6. PERFORMING ORG. REPORT NUMBER	
7. AUTHOR(s)	8. CONTRACT OR GRANT NUMBER(s) (15) N00024-75-C-5316
9. PERFORMING ORGANIZATION NAME AND ADDRESS Teledyne Ryan Aeronautical 2701 Harbor Drive San Diego, California 92112	10. PROGRAM ELEMENT, PROJECT, TASK AREA & WORK UNIT NUMBERS
11. CONTROLLING OFFICE NAME AND ADDRESS Department of the Navy Naval Sea Systems Command Washington, D.C. 20360	12. REPORT DATE (11) 25 April 1976
	13. NUMBER OF PAGES 53
14. MONITORING AGENCY NAME & ADDRESS (if different from Controlling Office) (12) 57p.	15. SECURITY CLASS. (of this report) Unclassified
	15a. DECLASSIFICATION/DOWNGRADING SCHEDULE

16. DISTRIBUTION STATEMENT (of this Report)

DISTRIBUTION STATEMENT A
Approved for public release;
Distribution Unlimited

17. DISTRIBUTION STATEMENT (of the abstract entered in Block 20, if different from Report)

18. SUPPLEMENTARY NOTES

19. KEY WORDS (Continue on reverse side if necessary and identify by block number)

Phased Array
IMPATT AM and FM Noise Analysis
Coaxial Interconnects
Interconnect Vibration and Temperature Data of Phase and Amplifude

20. ABSTRACT (Continue on reverse side if necessary and identify by block number)

The effort completed for this development contract consisted of two tasks. The first task was to conduct IMPATT transmitter spectral noise performance measurements and analyze the effects on active missile seeker performance. The second task was to develop an X-band, phased array, modular antenna manifold interconnection technology through the exploration of interface connection techniques at microwave frequencies.

DD FORM 1 JAN 73 1473 EDITION OF 1 NOV 65 IS OBSOLETE

Unclassified

SECURITY CLASSIFICATION OF THIS PAGE (When Data Entered)

389 357

TABLE OF CONTENTS

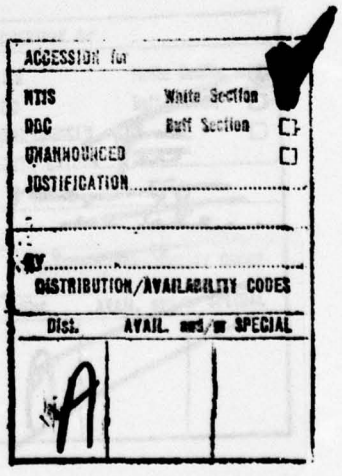

SECTION 1

INTRODUCTION

This Final Technical Report has been prepared in accordance with Item 0005 of NAVSEA Contract No. N00024-75-C-5316. The objective of this effort has been to continue the development of advanced missile seeker technology. This report documents the development effort that Teledyne Ryan Aeronautical has completed for the Naval Sea Systems Command from 1 August 1975 to 19 April 1976.

The effort completed for this development contract consisted of two tasks. The first task was to conduct IMPATT transmitter spectral noise performance measurements and analyze the effects on active missile seeker performance. The second task was to develop an X-band, phased array, modular antenna manifold interconnection technology through the exploration of interface connection techniques at microwave frequencies.

The summary of the overall requirements and effort is discussed in Section 2. A detailed technical discussion and description of test results and analysis is reported in Section 3. A technological forecast, which delineates technological problems, solutions and forecasts with their associated suggestions, recommendations, implications and conclusions is reported in Section 4.

SECTION 2

SUMMARY OF REQUIREMENTS

The scope of this program provided continued investigations, analyses and exploratory development of advanced missile seeker technology for a period of nine (9) months, beginning 25 July 1975, per the following detailed work description.

Task 1 of this program was the Spectral noise investigation of the IMPATT transmitter. This task was completed during the period 1 August 1975 to 1 January 1976 and included the following individual items:

- Construction of a test bench to measure AM and FM spectral performance of the IMPATT transmitter developed under contract no. N00017-74-C-4308.

- Measurement of the spectral noise characteristics of all three transmitter units versus input drive level, temperature and vibration.

- Analyze effects of the measured spectral noise components on the performance of an active, pulse doppler missile seeker.

Task 2 of this program was to develop X-band phased array module interconnect technology. This task was accomplished in five steps over the duration of the entire program from 1 August 1975 to 19 April 1976, and included the following individual items:

- Definition and specification of the microwave interconnection requirements:
  - VSWR
  - Insertion Loss
  - Power Levels
  - Allowable Phase Variations

- Definition of all possible environmental conditions for the microwave interface connection.

- Design, development, and construction of candidate interconnection techniques.

- Study and define production techniques needed to produce the best interconnection technique.

- Conduct a production cost analysis for the best interconnection technique.

Task 3 of this program was to provide a set of viewgraphs indicating technical objectives to be achieved, major milestones, schedules, approaches, block and schematic diagrams. This task was accomplished during the period 1 August 1975 to 15 September 1975 and delivered 1 October 1975.

Task 4 of this program was to prepare and furnish three (3) copies of each bimonthly technical letter progress report. Three bimonthly reports were prepared during the program and were furnished on 15 October 1975, 15 December 1975 and on 10 February 1976.

SECTION 3

DETAILED DISCUSSION

The program was divided into two major tasks. Details of each task are described in the following paragraphs.

3.1 TASK 1 - IMPATT TRANSMITTER SPECTRAL NOISE INVESTIGATION

An X-band IMPATT transmitter was developed by Teledyne Ryan for NSSC under Contract No. N00017-74-C-4308. The transmitter was developed in a Microwave Integrated Circuit (MIC) configuration for future use in an active, modular phased array antenna. A photograph of the transmitter is shown in Figure 1. A block diagram of the transmitter as well as the test configuration used to measure AM-FM noise spectra are shown in Figures 2 and 3.

The objective was to investigate the spectral noise performance of three transmitter breadboards, which had been previously fabricated and characterized, and to analyze the effects of this noise on the performance of an active missile seeker. The overall effort was accomplished in three sub-tasks.

3.1.1 Construct Test Bench

A block diagram of the test setup used for the FM and AM noise measurements is shown in Figure 3. The test bench was assembled and calibrated by substituting a known reference source. In this setup, the same signal was used for the LO as the amplifier drive, and is described as follows:

$$\text{LO} = [1 + B(t)] \sin [\omega t + \theta + C(t)]$$

$$\text{POINT A} = [1 + B(t)] \sin [\omega t + C(t)]$$

$$\text{POINT B} = [1 + B(t)] [1 + D(t)] \sin [\omega t + C(t) + E(t)]$$

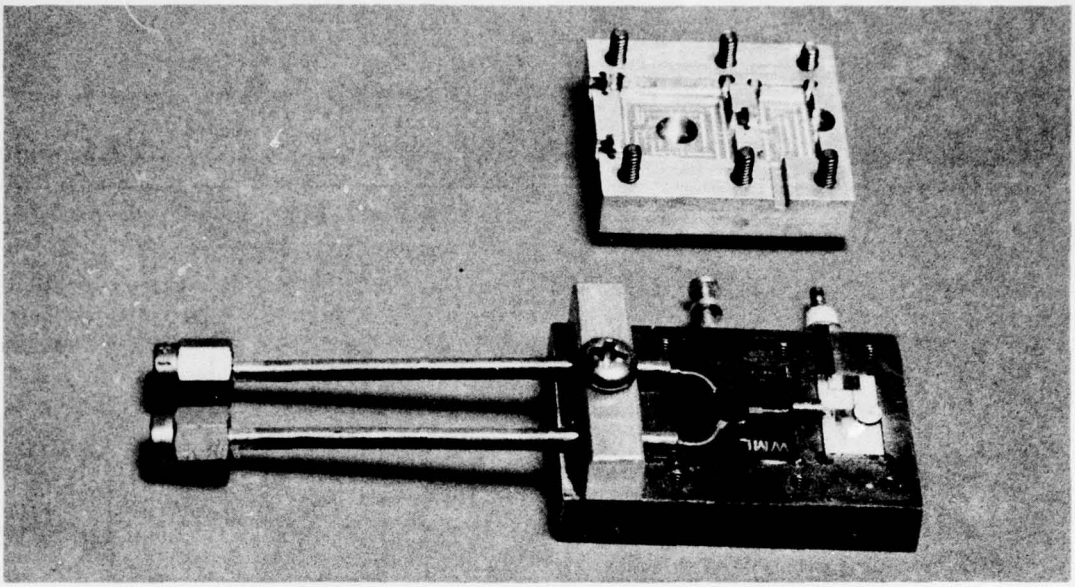

Figure 1. X-Band IMPATT Transmitter Developed by Teledyne Ryan Electronics and Used for Spectral Noise Investigation

where:

B(t) = klystron AM noise

C(t) = klystron FM noise

D(t) = IMPATT AM Noise

E(t) = IMPATT FM Noise

The mixer used was a Lunar Module (LM) low noise balanced mixer whose output can be represented as the product of the signal and LO', where

$$LO' = \sin [\omega t + \theta + C(t)]$$

The amplitude term of the LO is removed due to the AM balance of the mixer. The mixer output is then:

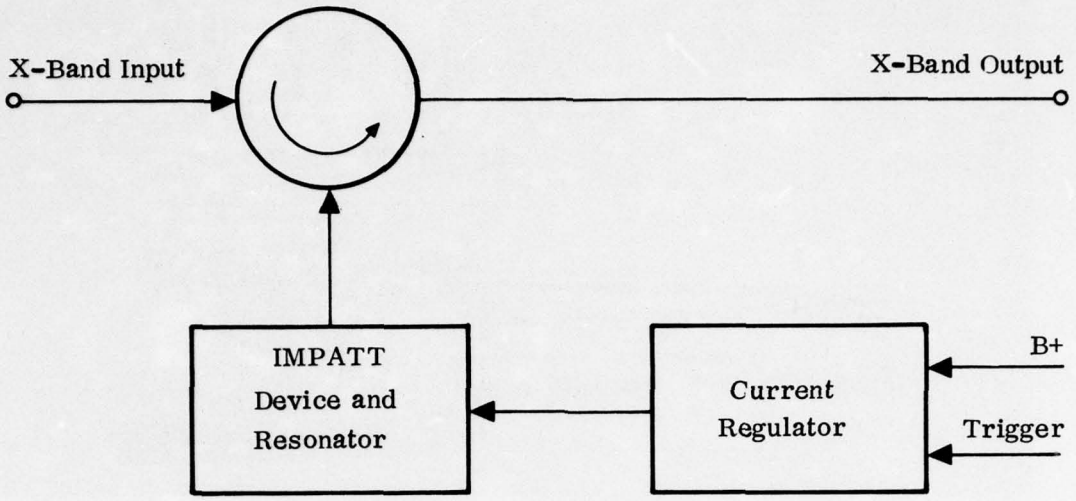

Figure 2. Block Diagram of X-Band, 1 Watt IMPATT Transmitter

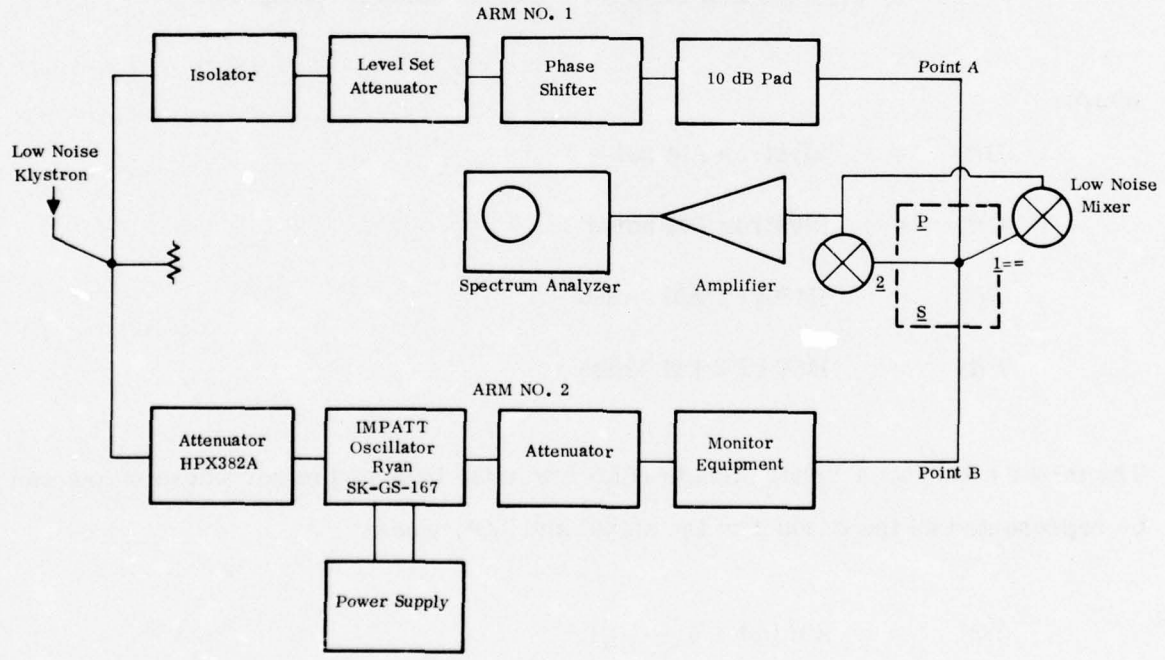

Figure 3. Block Diagram for IMPATT Oscillator AM-FM Noise Test

$$\text{Output} = [1 + B(t)] \quad [1 + D(t)] \quad \cos \quad [E(t) - \theta]$$
$$- [1 + B(t)] \quad [1 + D(t)] \quad \cos \quad [2\omega t + 2C(t) + E(t)]$$

The double frequency term at 20 GHz is filtered out leaving,

$$\text{Output} = \{1 + B(t) + D(t) + [B(t)\ D(t)]\} \cos [E(t) - \theta]$$

Since the AM terms B(t) and D(t) are small, the product B(t) D(t) can be disregarded, and

$$\text{Output} = [1 + B(t) + D(t)] \cos [E(t) - \theta]$$

Examining the output, it can be seen that if $\theta = 0$ the cos [E(t)] will be equal to 1, since the values of E(T) are very small. The output minus the dc term is the sum of the AM modulation of the klystron and IMPATT. When $\theta = 90^\circ$ the output is sin [E(t)] or equal E(t) since B(t) and D(t) are small compared to unity and can be ignored and E(t) is small; hence, the sin [E(t)] is approximately equal to E(t). This term is the FM noise of the IMPATT only.

Hence, by varying the phase of the LO it is possible to separate the FM and AM terms of the IMPATT noise. It is further possible to estimate the value of B(t) (klystron AM noise) by removing the IMPATT and measuring the AM noise of the klystron. In practice, this term is small and can be ignored and the experiment measures the AM and FM noise of the IMPATT under test.

The set was calibrated by replacing the signal with an independent oscillator of known power and measuring the spectrum analyzer response at the difference frequency. When this was done, the mixer conversion loss and miss-match losses were found to be 10 dB and the system gain from the signal input to analyzer was 40 dB.

The power from the signal generator was adjusted such that the voltage out of the amplifier is equal to -60 dBm. The spectrum analyzer was then calibrated.

The noise level with respect to the carrier is given by:

$$\frac{\text{noise}}{\text{carrier}} = \frac{\text{analyzer reading}}{\text{carrier reading}} - 40\ \text{dB} - 6\ \text{dB}$$

where 40 dB is the system gain and 6 dB accounts for the double sideband nature of the noise versus the desired single sideband measurement.

Since the noise is of double sideband nature, the beating to zero folds the desired spectrum on itself and doubles the voltage compared to the desired single sideband measurement; hence, the 6 dB factor.

The test setup is basically a microwave phase bridge consisting of two arms driven by the same source.

Arm no. 1 consists of a phase shifter , 10 dB pad and level set attenuator. Arm no. 2 consists of attenuators, IMPATT diode injection lock oscillator, and monitoring equipment, such as frequency meter, spectrum analyzer, power meter, etc. Both arms are then applied to a double balanced mixer.

The local oscillator (Arm no. 1) was applied to one port and the second arm was applied to the other.

The signal generator was removed and replaced with the second arm. The power level was set to -15 dBm, and injection locking power to 100 milliwatts. The phase bridge was balanced by removing the amplifier from the balanced mixer, connecting a dc voltmeter and adjusting the phase shifter to null the dc voltage. The phase shifter was set to zero phase.

The oscilloscope was then removed and replaced with the amplifier and spectrum analyzer. The spectrum analyzer response is the IMPATT FM noise. This information was stored on the analyzer. The phase shifter was rotated 90° and another plot taken. This is the IMPATT AM noise. This information was also stored. The power into the balanced mixer was removed and terminated. A plot of this data was made. This is the system noise. The combined data was recorded by photographing the spectrum analyzer display.

An example of the spectrum analyzer photogarphs are shown in Figure 4. The spectrum analyzer was operated using the narrowest band, 10 Hz, video filter in order to decrease the amplitude variation in the data. The variable persistance memoscope was set for infinite storage such that three successive spectral traces could be made.

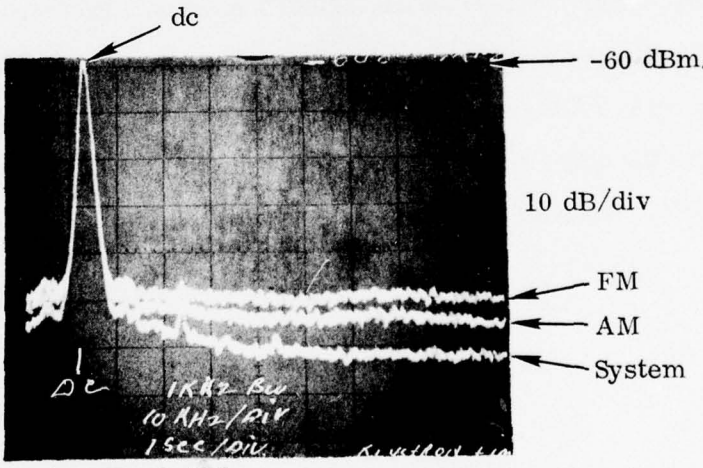

Figure 4. Example of Spectrum Analyzer Photographs used for Spectral Noise Evaluation and Data Reduction

3.1.2 Measured Spectral Noise Characteristics of IMPATT Transmitter

A photograph of the three transmitters and an associated current regulator breadboard used to conduct the spectral noise measurements is shown in Figure 5. The measured noise level 5 kHz and larger from the carrier was -100 dBc for FM noise and -110 dBc for AM noise in a 1 kHz bandwidth. The resultant data for the two IMPATT transmitters tested is summarized in Figures 6 through 11.

The third IMPATT was tested and the results were much worse than the other units. The FM noise level was -91 dBc and the AM noise level was -105 dBc. Troubleshooting revealed that the unit had poorer performance due to very low input locking power. Before this discrepancy was noticed, the unit failed and no further data could be taken.

Additional data was taken on the remaining units under vibration by using a hand-held vibrator and accelerometer mounted on the IMPATT housing. No increase in noise level was evident for sine wave of levels up to 3g peak-to-peak from 0 Hz to 2.5 kHz. For frequencies above 2.5 kHz, no increase was evident for 1g levels at 10, 17, and 30 kHz. These were the only frequencies at which the vibrator could be resonated at greater than 1g levels. Over all, the units exhibited good stability during the brief vibration tests.

The oscilloscope was then removed and replaced with the amplifier and spectrum analyzer. The spectrum analyzer response is the IMPATT FM noise. This information was stored on the analyzer. The phase shifter was rotated 90° and another plot taken. This is the IMPATT AM noise. This information was also stored. The power into the balanced mixer was removed and terminated. A plot of this data was made. This is the system noise. The combined data was recorded by photographing the spectrum analyzer display.

An example of the spectrum analyzer photogarphs are shown in Figure 4. The spectrum analyzer was operated using the narrowest band, 10 Hz, video filter in order to decrease the amplitude variation in the data. The variable persistance memoscope was set for infinite storage such that three successive spectral traces could be made.

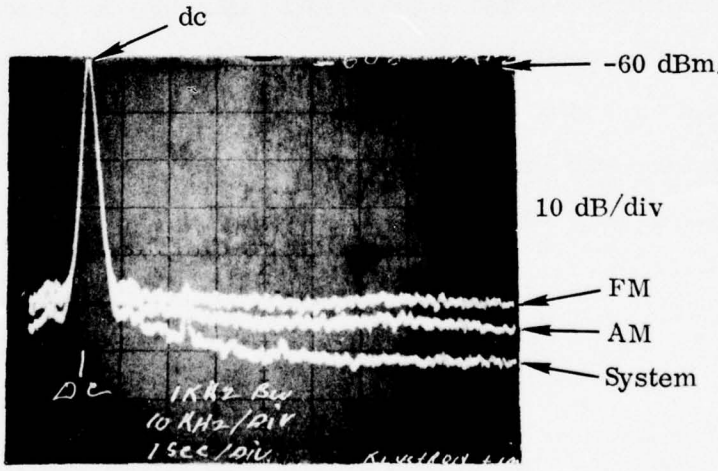

Figure 4. Example of Spectrum Analyzer Photographs used for Spectral Noise Evaluation and Data Reduction

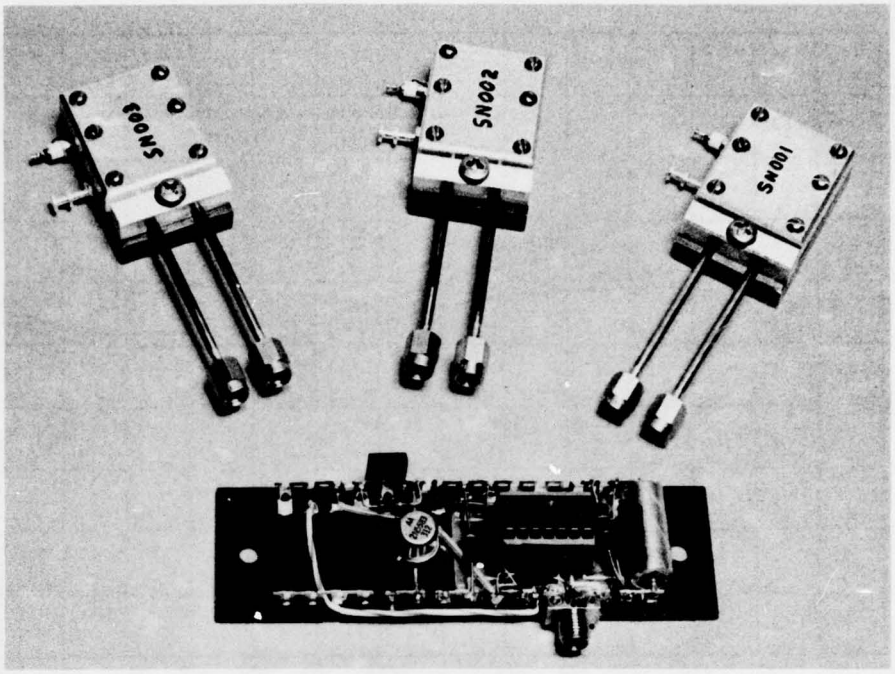

Figure 5. Three IMPATT Transmitter Units and Current Regulator Breadboard used in Spectral Noise Measurements

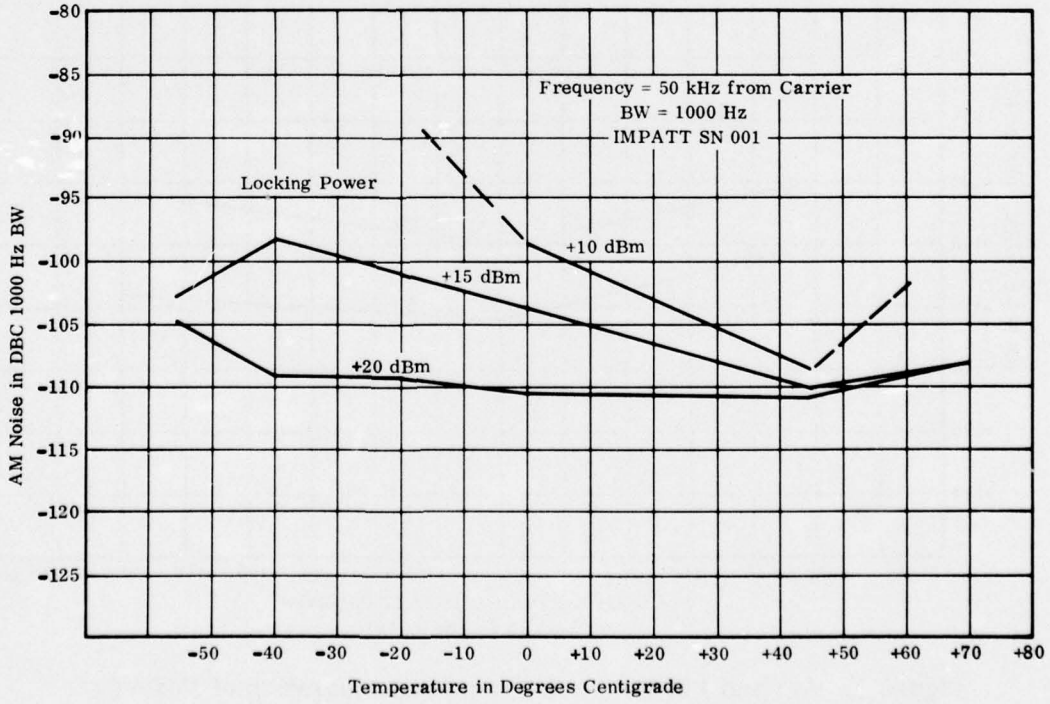

Figure 6. AM Noise vs Temperature

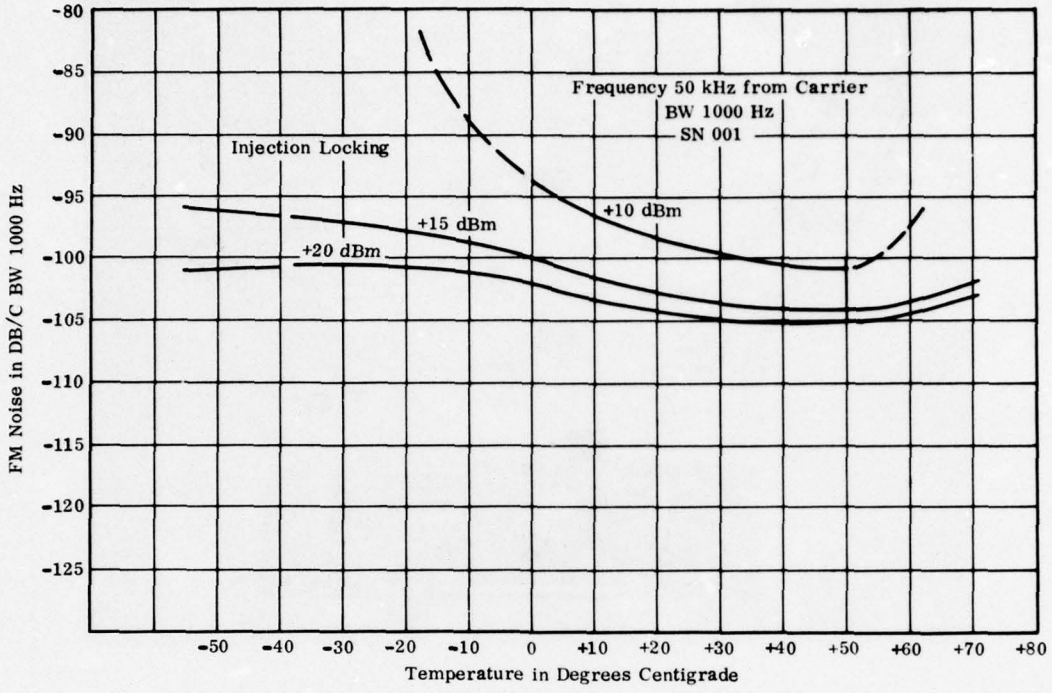

Figure 7. FM Noise vs Temperature

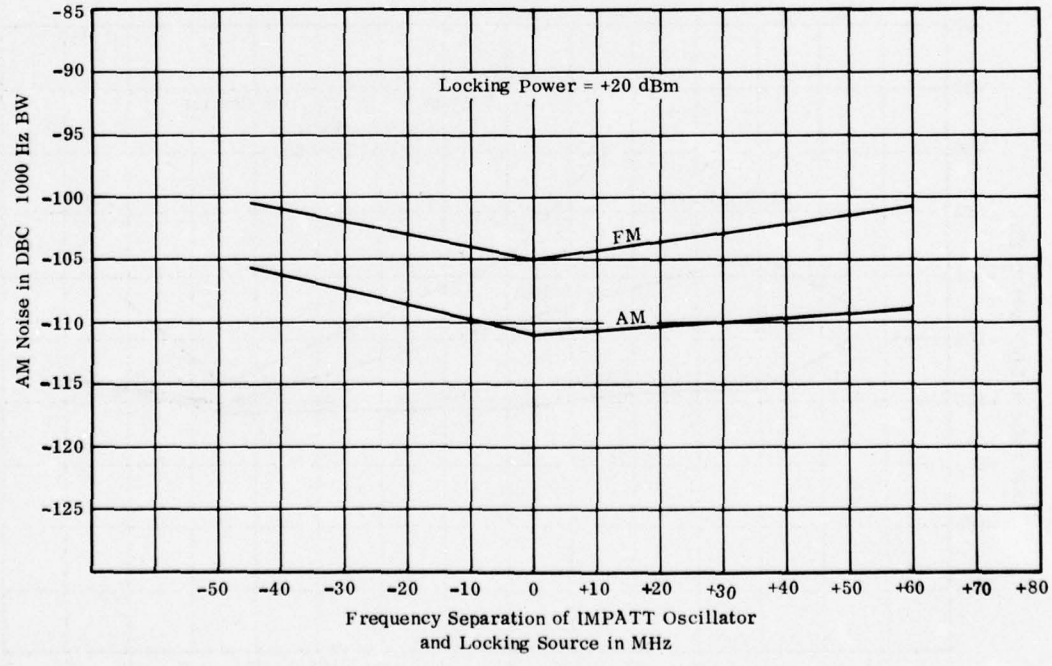

Figure 8. AM and FM Noise vs Frequency Separation of IMPATT Oscillator and Locking Source

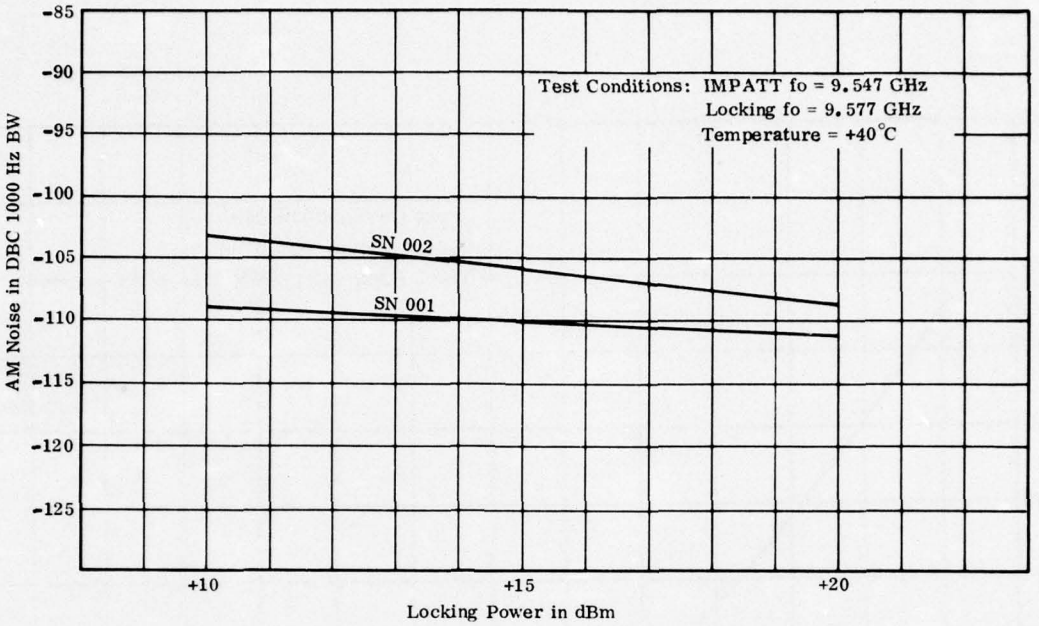

Figure 9. AM Noise vs Locking Power

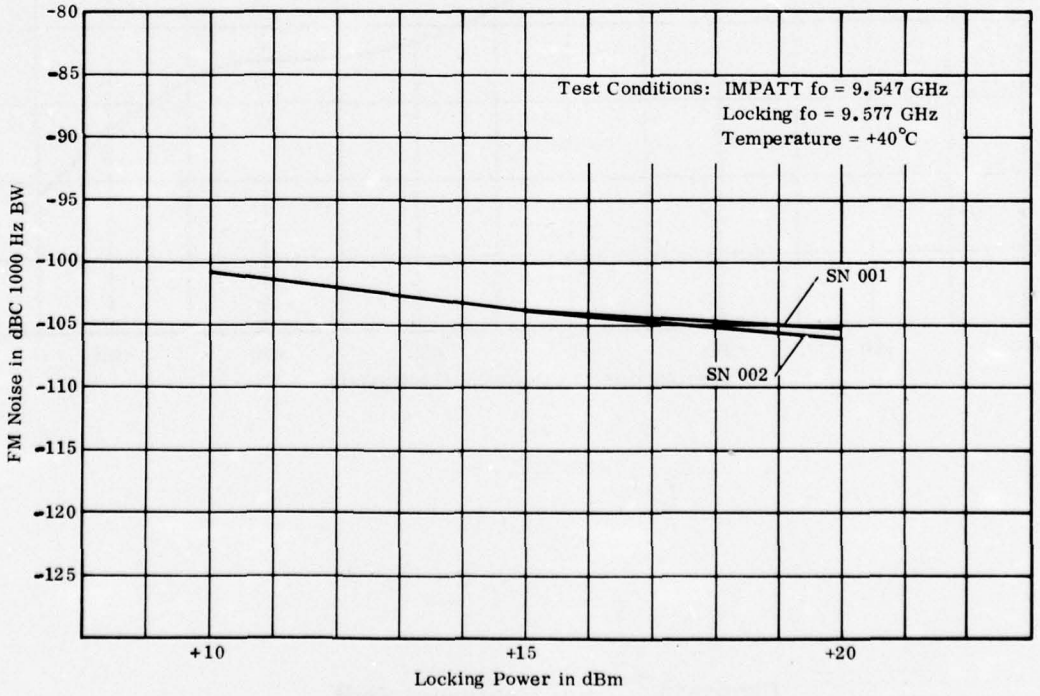

Figure 10. FM Noise vs Locking Power

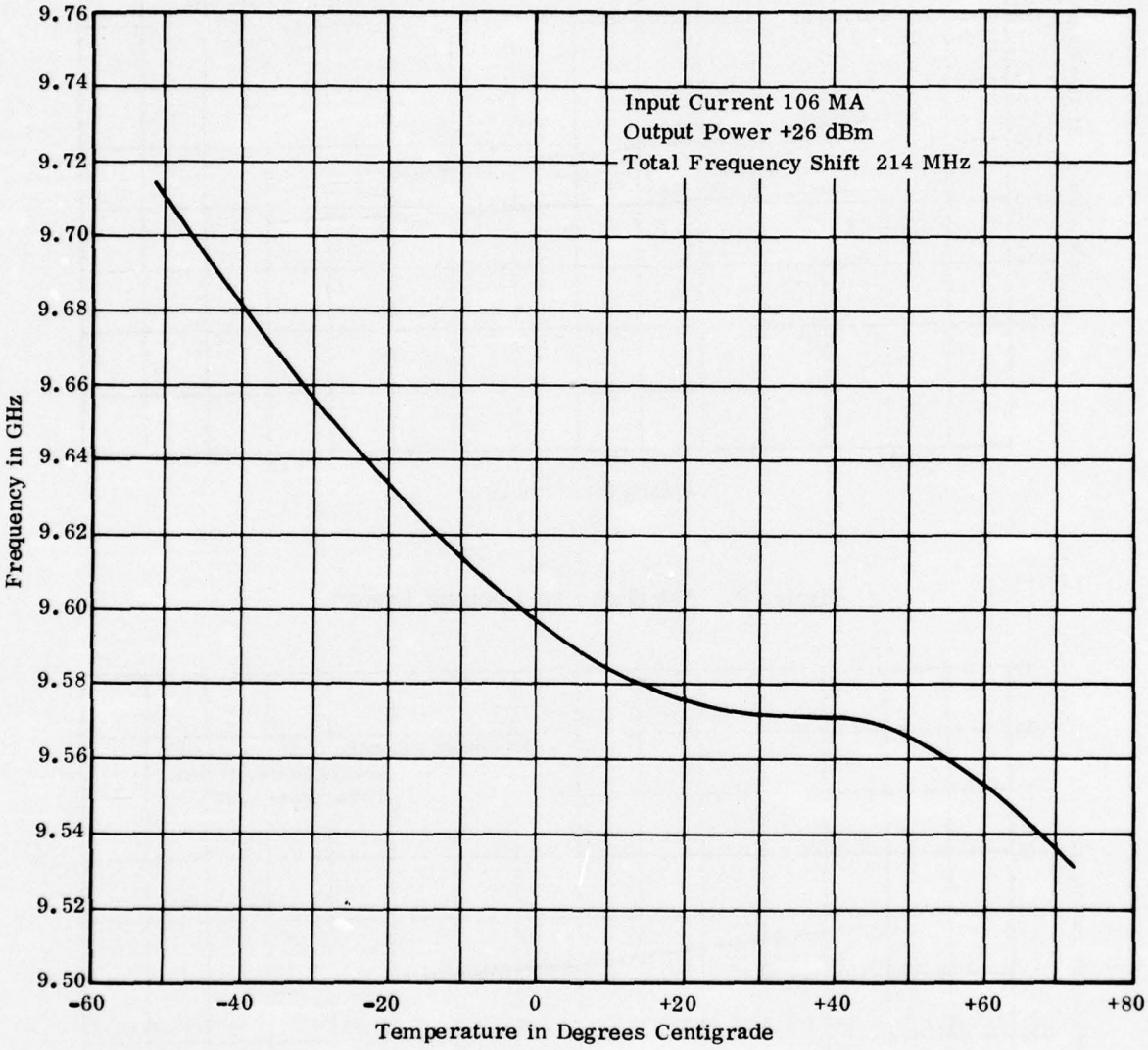

Figure 11. Total Frequency Shift

3.1.3 Analyze Noise Effects on Active Seeker Performance

Analyses to define the effects of the measured noise characteristics on a typical active missile seeker were completed.

The conclusion drawn from this analysis is that the IMPATT amplifiers have very good spectral noise performance over both temperature and vibration. The measured FM noise level of -100 dBc in a 1 kHz bandwidth greater than 5 kHz removed from the carrier should be completely adequate for any of the currently proposed active phased array seeker systems operating in the worst realistic value of clutter return, specifically 1000 foot level flight over wooded terrain with close-in antenna sidelobes of 20 dB.

The required FM-AM noise levels for the transmitter are defined by the total returning clutter power and the receiver noise level since the noise in the clutter (transmitter) sidebands must be below the receiver noise so as not to degrade the system noise figure. The main source of the returning clutter energy is the main beam clutter at which frequencies the system cannot track any targets. However, the clutter power times the sideband level cannot be so large as to raise the noise level for frequencies away from the main beam clutter and degrade system performance. This relationship is given below:

$$S \leq \frac{kT\,B\,F}{P\,C\,M}$$

where:

S = single sideband (FM + AM noise level in bandwidth B)/carrier ratio

kT = reference noise density

B = receiver noise bandwidth

F = receiver noise figure

M = margin factor (receiver noise/clutter noise)

P = transmitter power

C = fraction of transmitter power returned to receiver as clutter

A computer program was written which calculates the factor C for a seeker system given σ_o and the system antenna patterns and trajectories. This program also calculates the spectrum of the returning energy for sidelobe clutter calculations.

The worst realistic value of C was -112 dB for 1000 foot level flight over wooded terrain with close-in sidelobes of 20 dB. This should be a worst case situation since the value will decrease for higher altitudes and other surface backscatterers (desert, sea, etc.). Using this value, the sideband levels are calculated below:

Parameter		10 Log Value
kT		-204
B	1000 Hz	+30
F	Noise Figure	+7
P	250 Watts	-24
M	Margin 10 dB	-10
C		+112
S	Transmitter Noise Level/kHz with Respect to the Carrier	-89 dBc

3.2 TASK II - DEVELOP X-BAND, PHASED ARRAY MODULE INTERCONNECT TECHNOLOGY

Acceptable interconnections for interchangeable X-band phased array antenna modules were not available. Also, military specifications are not known to exist for this requirement. Consequently, a development program was conducted to develop X-band interconnections which could be used in the production of phased array missile seekers.

3.2.1 Define Interconnection Requirements

Electrical and environmental requirements were defined prior to the development of X-band interconnections. Military Specification MIL-C-39012/Series SMA for SMA connections was studied for background information. SMA connectors are too large for this X-band module requirement. Additional requirements were considered to those listed in MIL-C-39012. A list of the electrical and environmental requirements is included in Table 1.

3.2.2 Development X-Band Module Interconnections

3.2.2.1 Mechanical Configurations. The first candidate X-band interconnection concept utilized two centering and aligning dowell pins which were orthoganally oriented with respect to two 50 ohm diagonally located coaxial connectors and form fastening screws. A sketch showing the concept is depicted in Figure 12.

A modification was made to simplify the original configuration. A single dowel centering pin was utilized in conjunction with only two diagonally located fastening screws which are orthoganally located with respect to two OSSM type connectors. A sketch is shown in Figure 13 and photographs showing an end view of the module and module receptacle are shown in Figures 14 and 15. The connectors are held in compression by the use of a Bellville tension washer.

3.2.2.2 Connector Durability Tests. Tests were conducted with the modified configuration to determine relative phase and amplitude variations at room temperature as a function of connecting and disconnecting the connector 500 cycles. Measurements were conducted at three test frequencies to demonstrate the bandwidth performance of the connection. The results of the room temperature tests are shown in Figure 16.

Table 1. X-Band Interconnection Requirements

1.	VSWR	
	Maximum 1.15:1 for 500 Connections	
2.	Insertion Loss	
	0.15 dB Maximum for 500 Connections	
3.	Power Levels	
	Maximum 12.5 Watts, at Sea Level, Including all Microwave, RF, and dc Power	
4.	Transmission Phase Variation	
	(a) $\pm 10^{\circ}$ Maximum Repeatability for 500 Connections	
	(b) $\pm 2^{\circ}$ Variation vs. Temperature and Frequency for Each Connection	
5.	Frequency	
	10% Total Microwave Bandwidth on all Requirements	
6.	Leakage	
	-90 dB Maximum (Temporary, subject to review)	
7.	Missile Skin Temperature (Max)	$+275^{\circ}$F to -35°F
8.	Inner Missile Ambient Temp. (Max)	$+160^{\circ}$F to -35°F
9.	Vibration	$0.04g^2$/cps from 10 to 2000 cps
		$0.35g^2$/cps for 30 seconds (Frequency per a chart)
10.	Shock	50g longitudinal
		Rate, 35g/millisecond for 5 milliseconds

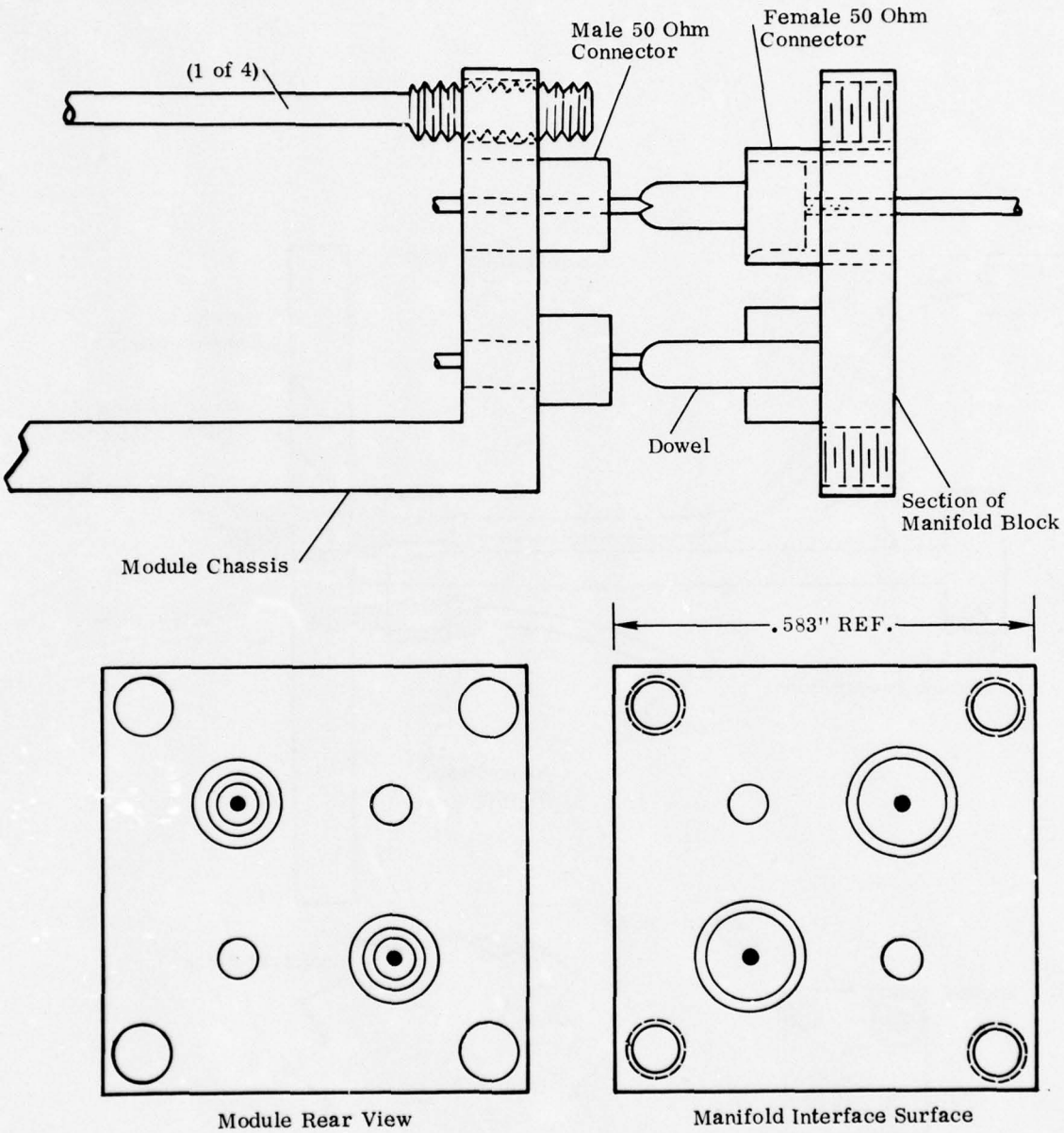

Figure 12. Sketch of Candidate X-Band Interconnection Configuration

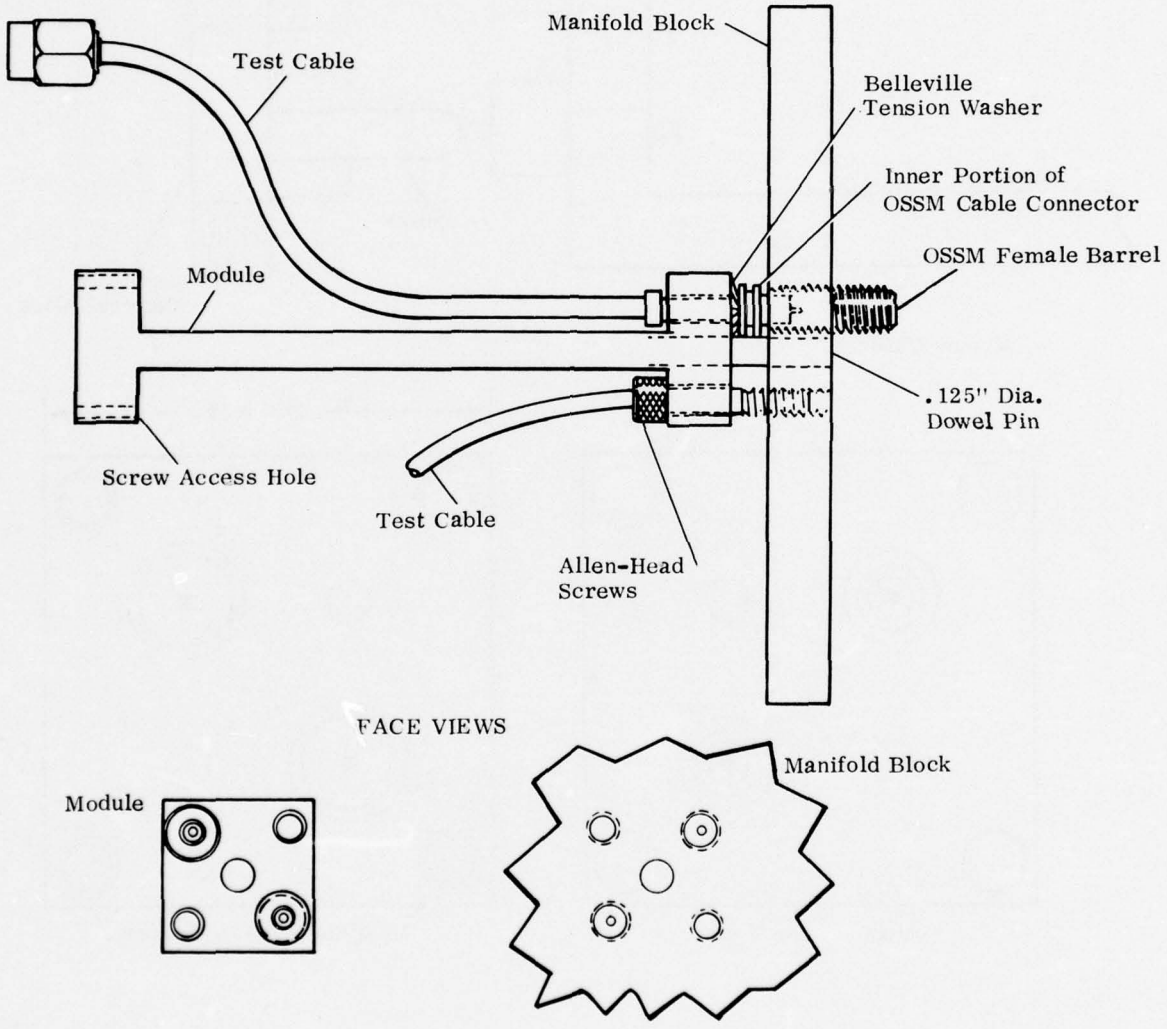

Figure 13. Sketch of X-Band Interconnection Configuration

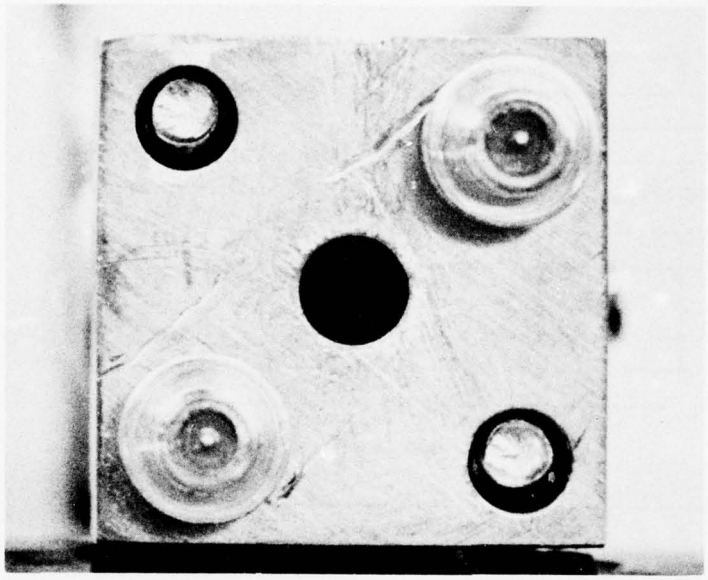

Figure 14. End View of Module

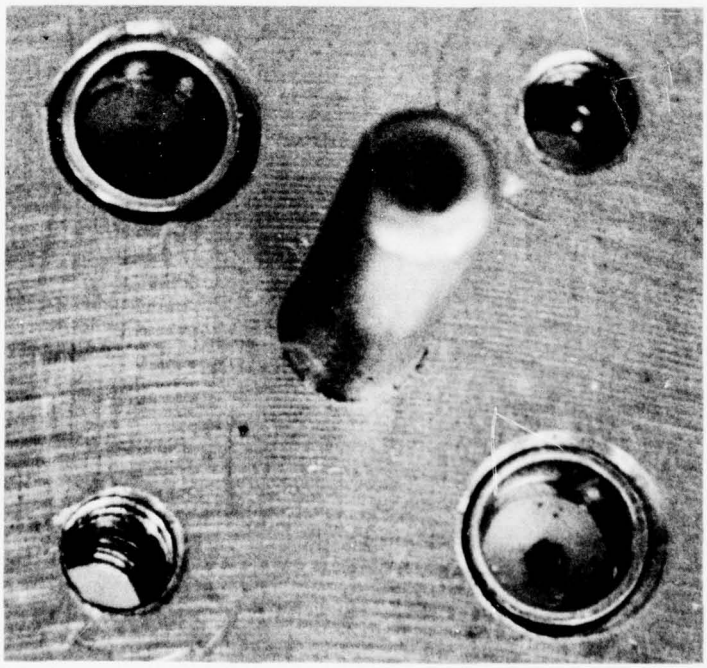

Figure 15. Module Receptacle

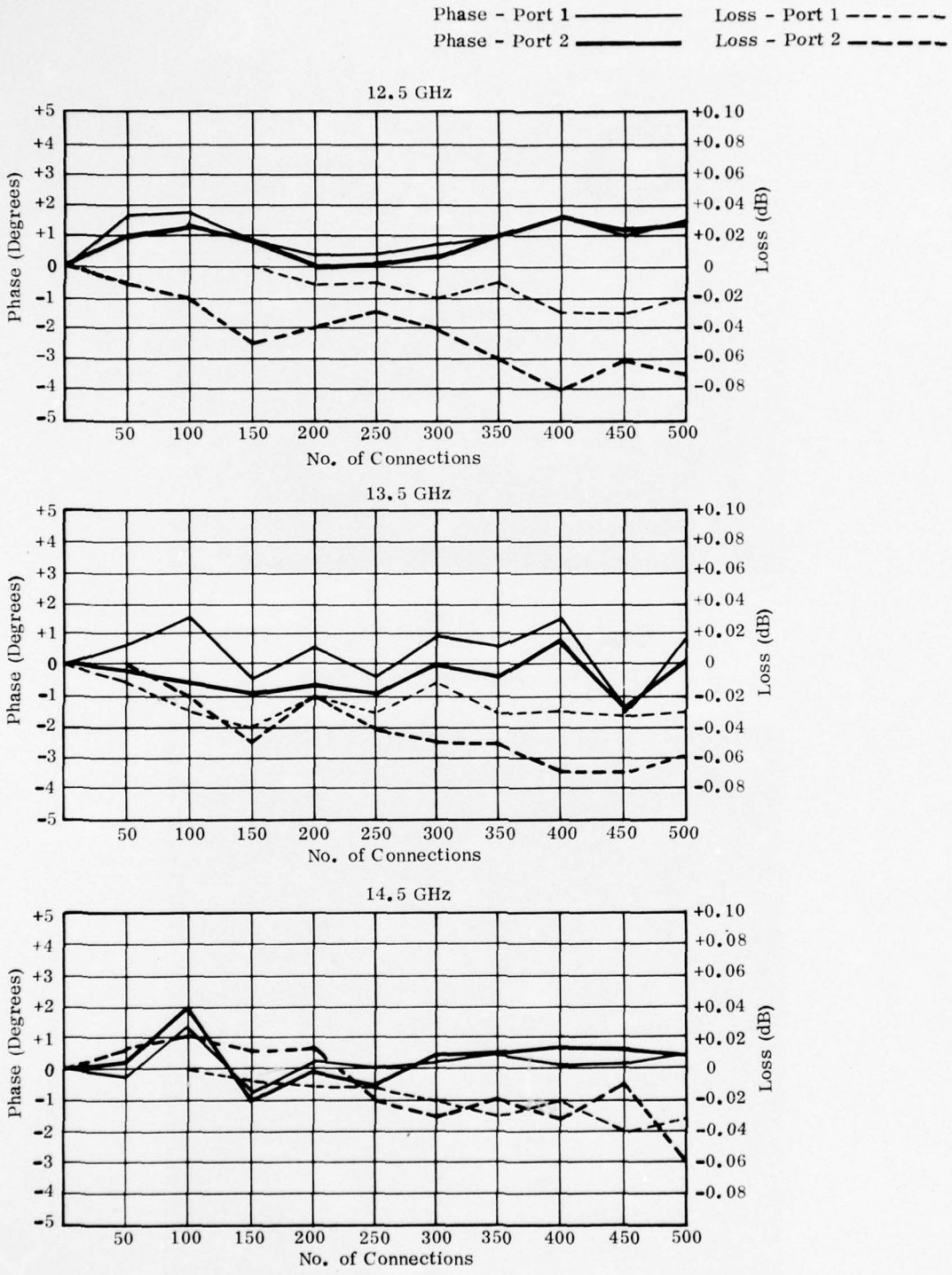

Figure 16. X- Band Interconnect, Phase and Amplitude Performance

3.2.2.3 Temperature Performance. The prototype connector, was subjected to temperature tests, where phase of the signal through the connector was measured as a function of temperature. Phase tests were chosen as the criterion of performance since this parameter is paramount in scanning phased array antennas. The test set-up used is shown in Figure 17. For convenience, tests were performed at 13.3 GHz, the results being applicable to lower frequencies as well.

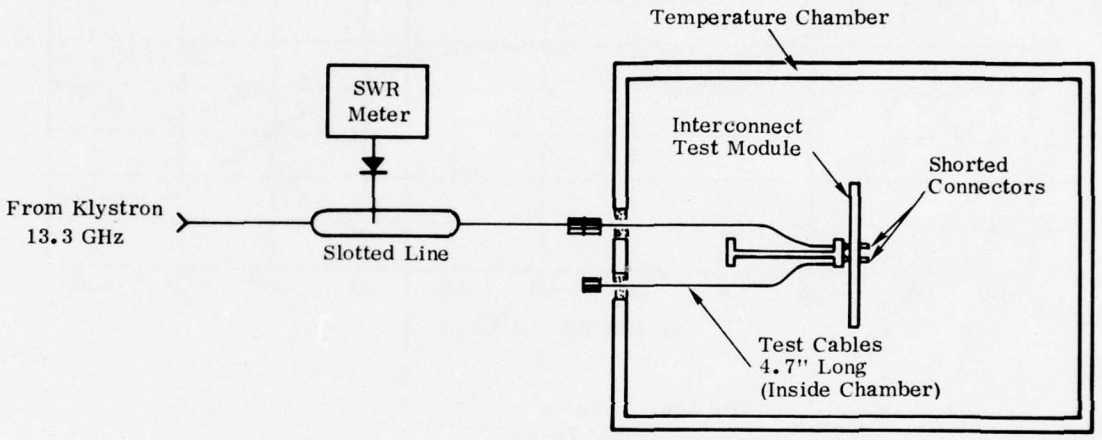

Figure 17. Temperature Test Setup

The temperature portion of the environmental tests required considerable test time. The major problem encountered was the isolation of the magnitude of various temperature dependent portions of the test setup, such that a quantitative evaluation of the connector under test could be realized.

Figure 18 shows the variation in the transmitted phase through each test connector versus temperature, with the other temperature dependent component contributors, such as the semi-rigid coaxial cable, removed. Also shown is the differential phase variation between the two connectors under test. This parameter, differential phase shift, is most important in the operation of a phased antenna array.

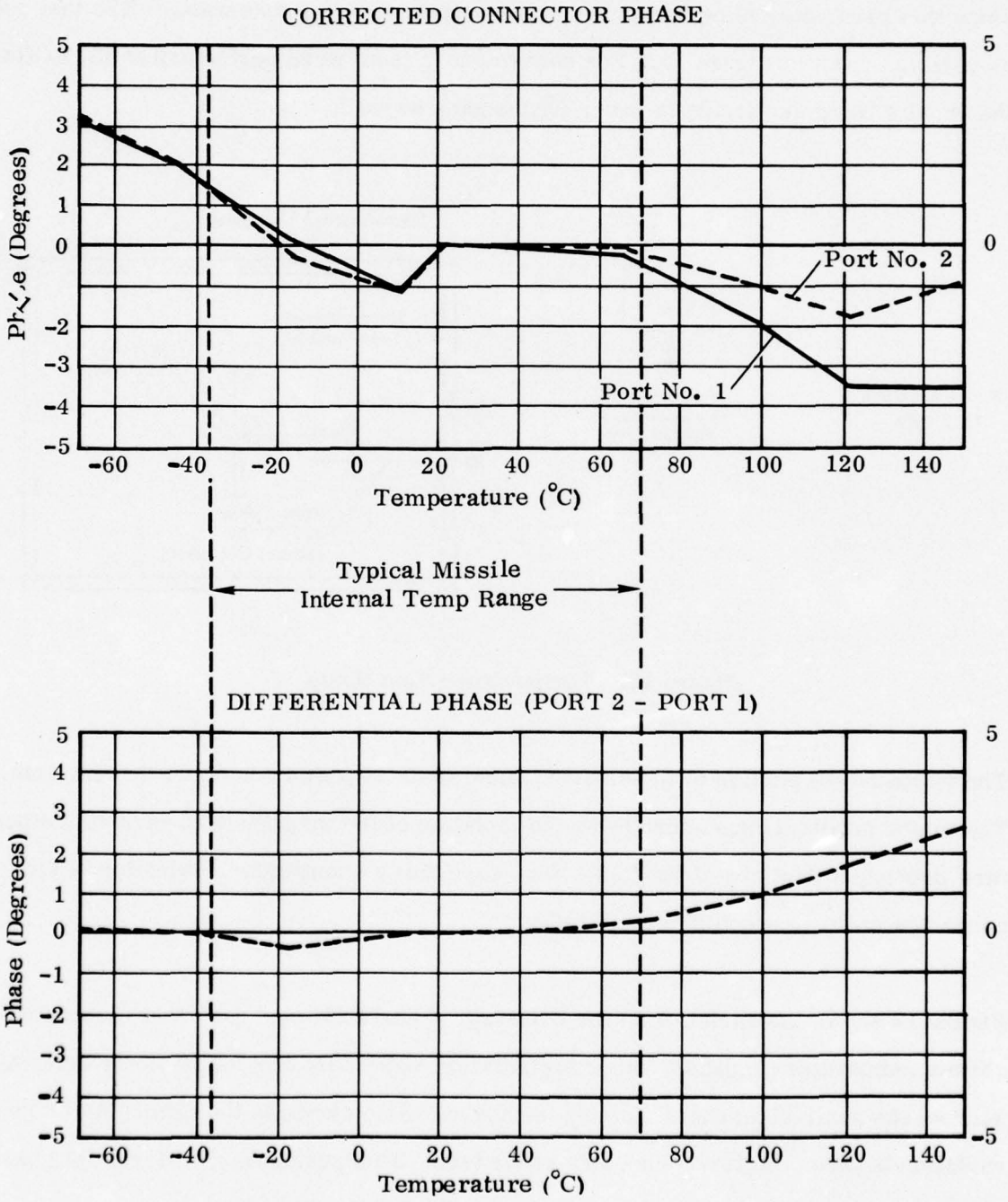

Figure 18. Phase vs. Temperature

Using the slotted line, the null position produced by the shorted output connectors on the test module was plotted as a function of chamber temperature. This test was performed on both ports of the interconnect test module. These null positions could be related to the phase of the signal through the test connectors. Since the 4.7 inch long semi-rigid coaxial test cables were also in the temperature chamber it was necessary to compensate for their phase/temperature sensitivity so that the connector phase could be separated from the total measured phase. Since the test cables were fabricated at room temperature (22°C) where the dielectric fills the cable, it was necessary to compensate for the phase error introduced at cold temperatures, where the dielectric recedes from the connector face. A discussion of these effects of provided in Appendix A.

3.2.2.4 Vibration Performance. A special vibration test fixture was designed and fabricated, and vibration susceptibility tests were conducted. A sketch of the vibration fixture is shown in Figure 19 and Figure 20 shows the Interconnect Module mounted for vibration tests. The small cylinder that is fastened to the vibration base block is an accelerometer, which is used for monitoring actual vibration levels, and for providing vibration feedback control.

The test equipment used to evaluate the Interconnect Module during vibration is depicted schematically in Figure 21 and photographically in Figure 22. This setup allows measurement of the phase amplitude of a microwave signal as it passes through the interconnect. The phase and amplitude signals are recorded for long periods with the "X - Y" Plotter, while short term vibration responses are photographed from the oscilloscope face. Electrically, the test setup is composed of a microwave bridge, with the Interconnect Module lying in the test arm. During vibration, the phase vibrations resulting from the Interconnect Module cause a proportional change in the level detected by the diode at the waveguide "Tee". This dc level change is recorded by the plotter and scope. For amplitude changes in the Interconnect Module during vibration, the detector is connected via the coaxial cable directly to the module, and the corresponding level changes are recorded.

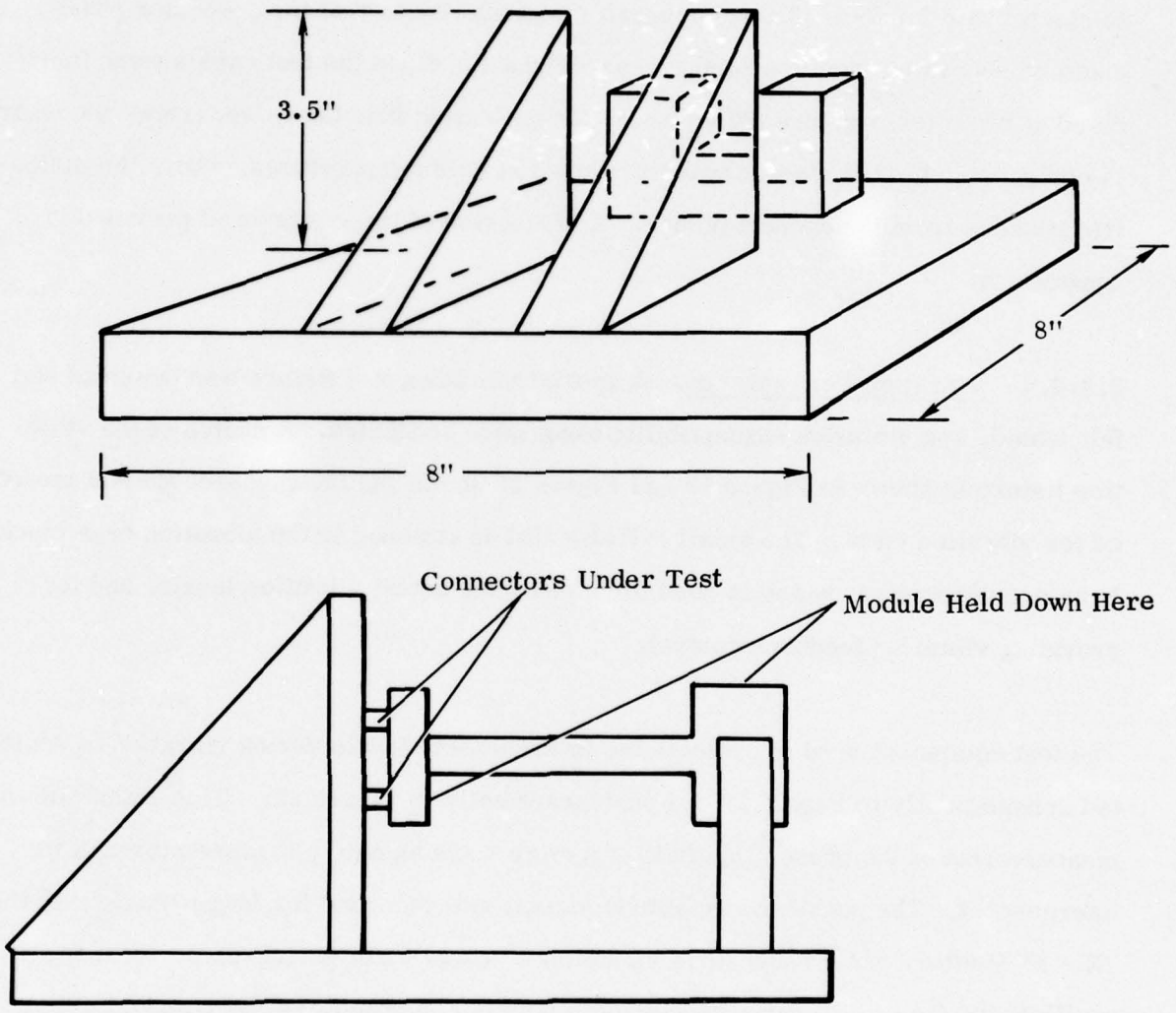

Figure 19. Vibration Test Fixture

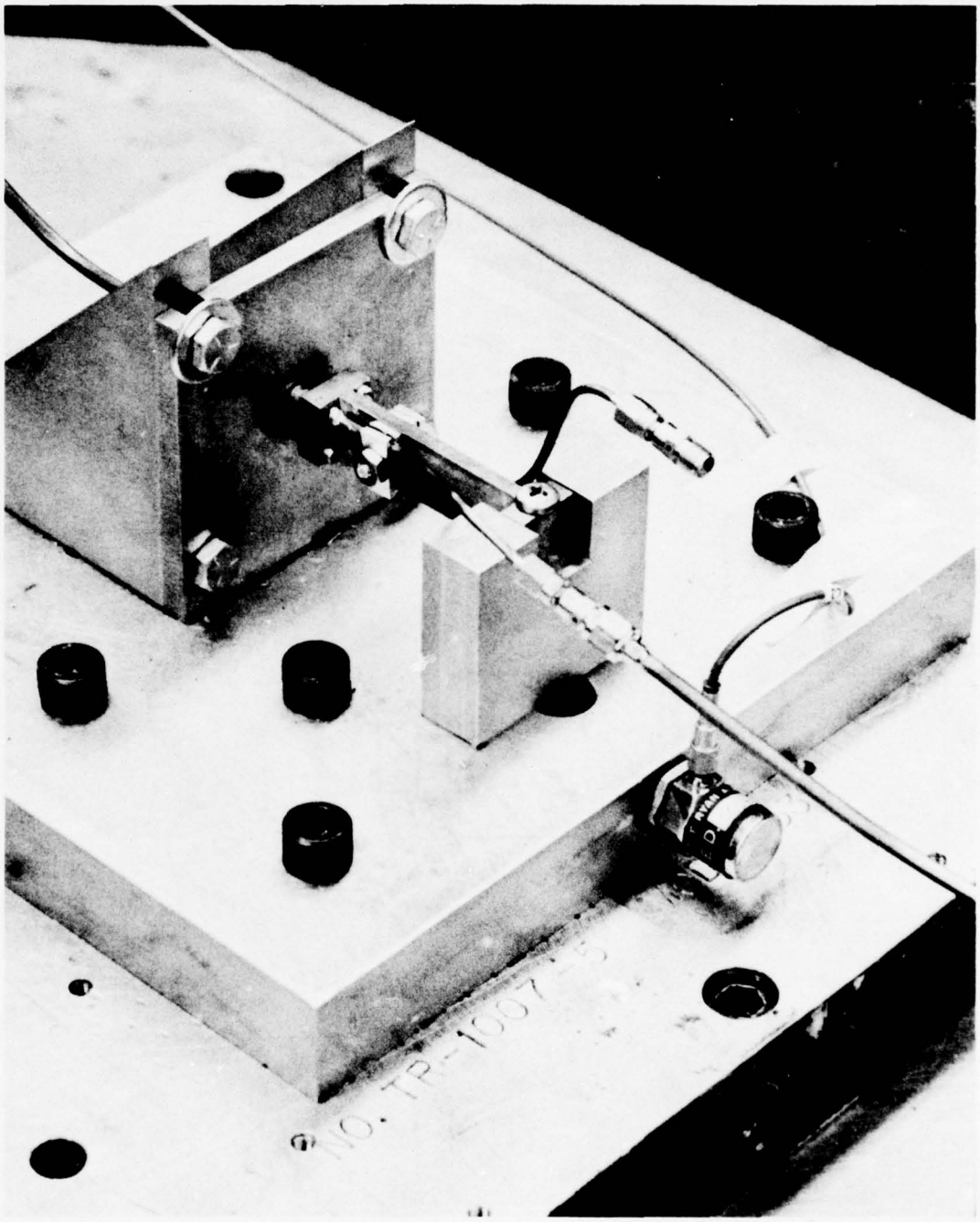

Figure 20. Interconnect Module Mounted for Vibration

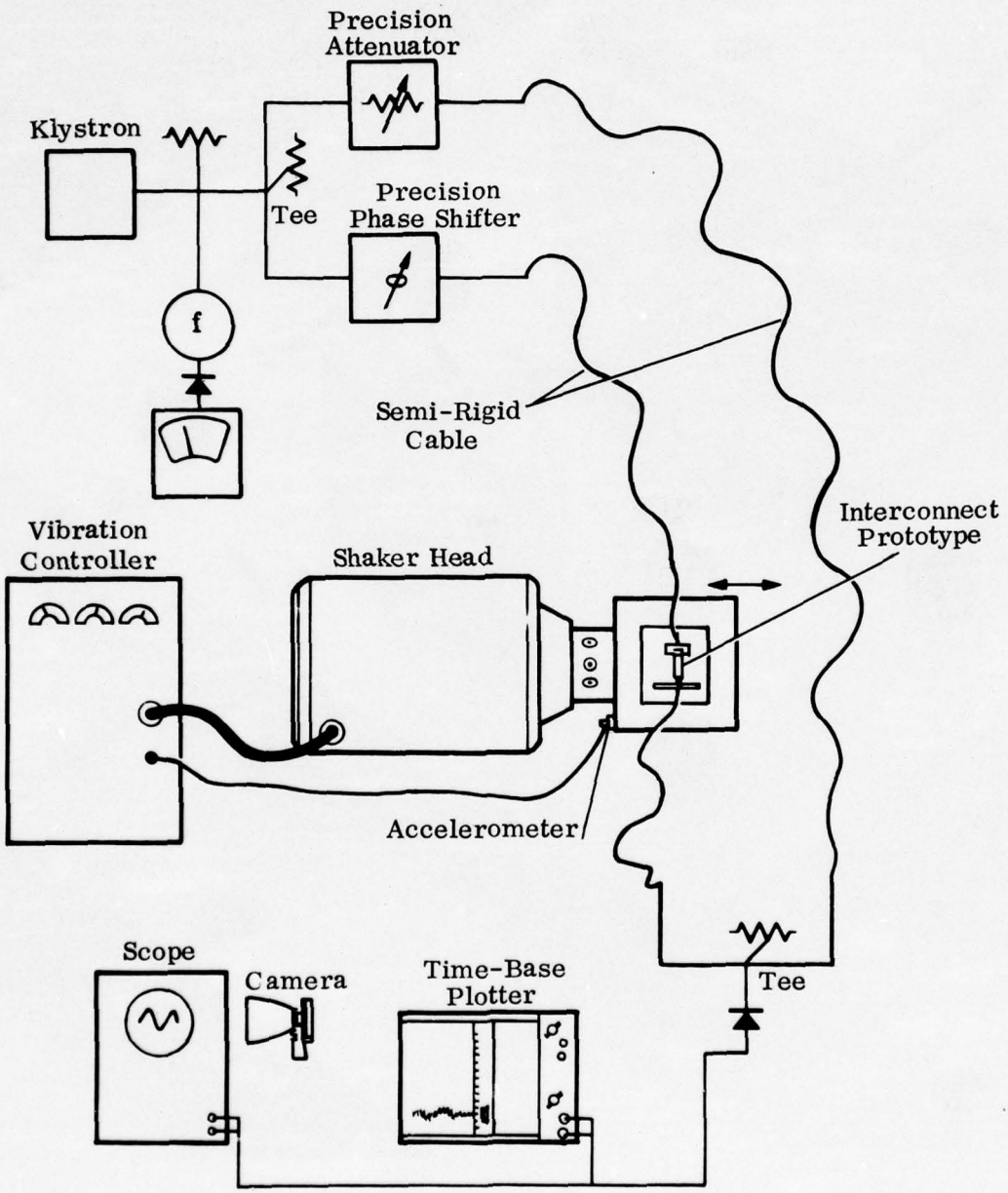

Figure 21. Vibration Test Setup

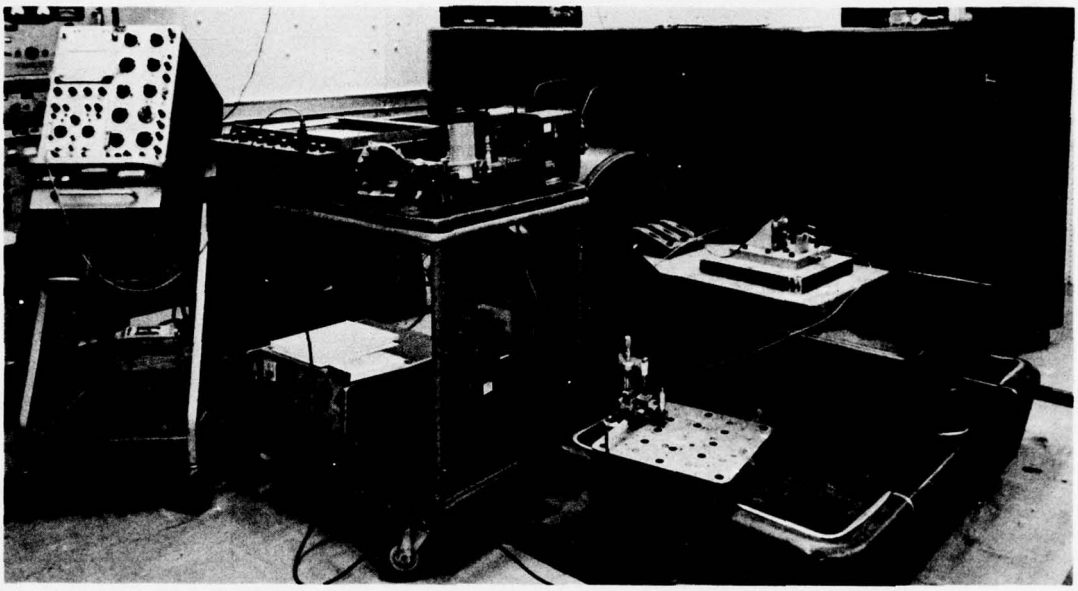

Figure 22. Test Equipment used for Vibration

The vibration levels chosen for these tests are based on typical missile applications. A level of 21g rms for 30 seconds was used to represent the launch and powered phase of missile flight. Nonpowered flight is represented by a vibration level of 8g rms for 5 minutes. A frequency range for the random vibration was set at 20 to 2000 Hz. Figure 23 depicts the actual levels obtained, as a function of frequency, for both levels of vibration. This information was recorded from the accelerometer that is mounted on the vibration block.

Two axes of vibration tests were performed. The longitudinal axis is along the direction of power flow in the connector. Latitude is perpendicular to this axis. Since the Interconnect Module is symmetrical in latitude, it is not necessary to perform vibration tests in a third axis.

Vibration tests were conducted on both ports number 1 and number 2 of the Interconnect Module along the longitudinal and lateral axes. An example of the typical long

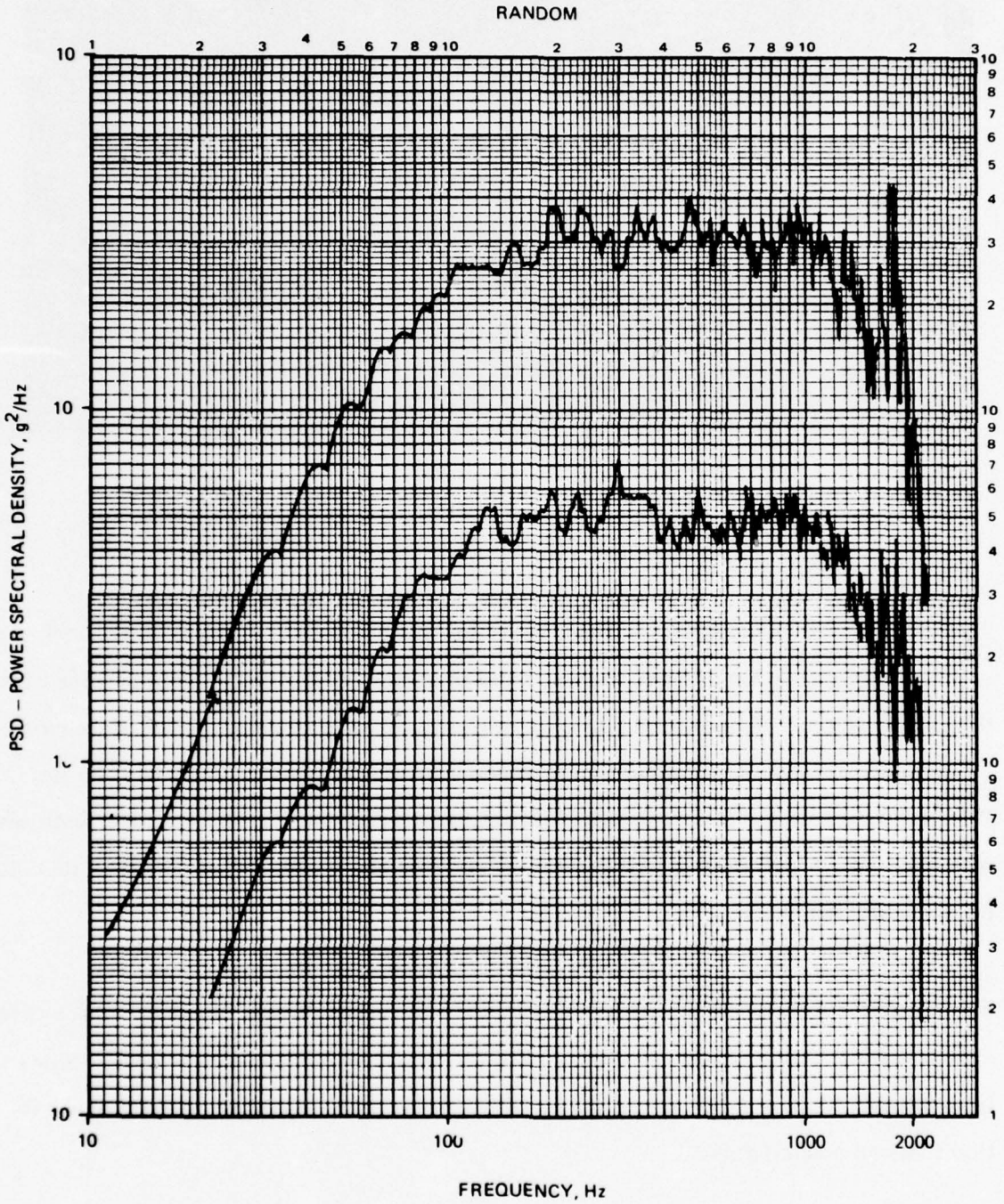

Figure 23. Actual Vibration Levels Obtained

term phase measurements for both levels of vibration is shown in Figure 24. An illustration of the oscilloscope presentation of typical short term phase changes during both levels of vibration is shown in the PHASE portion of Figure 25.

There are no large spikes in the short term phase responses and the peak phase variations are 0.15° for the 8g rms level and 0.20° for the 21g rms level. These results indicate acceptably low levels of phase change for both short term fluctuations, and long term drift.

Amplitude, or insertion loss, variations measured on the Interconnect Module are small enough for most system applications. The typical long term insertion loss changes measured for the two vibration levels is shown in Figure 26. The 21 g rms vibration level causes a peak amplitude change of 0.03 dB in 30 seconds, with 0.08 dB of total insertion loss for 8g rms vibration during a 5 minute period. An illustration of the oscilloscope presentation of short term amplitude variations of 0.005 dB for 8g rms vibration and 0.008 dB for 21g rms is shown in the INSERTION LOSS portion of Figure 25. Magnitudes of this order are entirely acceptable for most system types and modulation schemes. For systems operating within a few kHz of the carrier, such as "zero IF" Doppler systems, some degradation in performance on receiver input ports might be encountered during high vibration. Further work on this aspect would be required if this application were anticipated.

There were no general, or catastrophic failures, either electrical or mechanical, during the entire vibration test program.

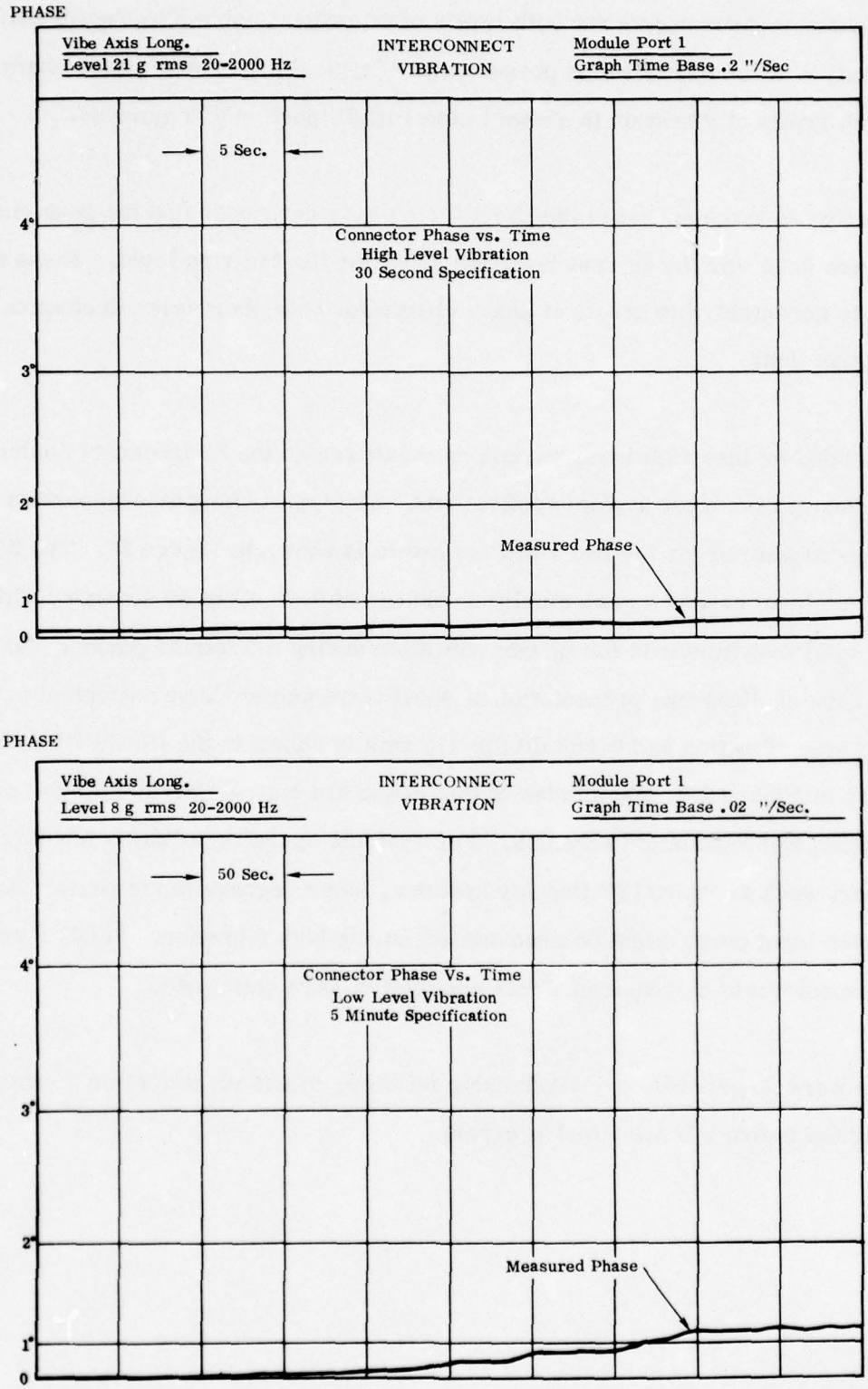

Figure 24. Long Term Phase Measurements During Vibration

PHASE

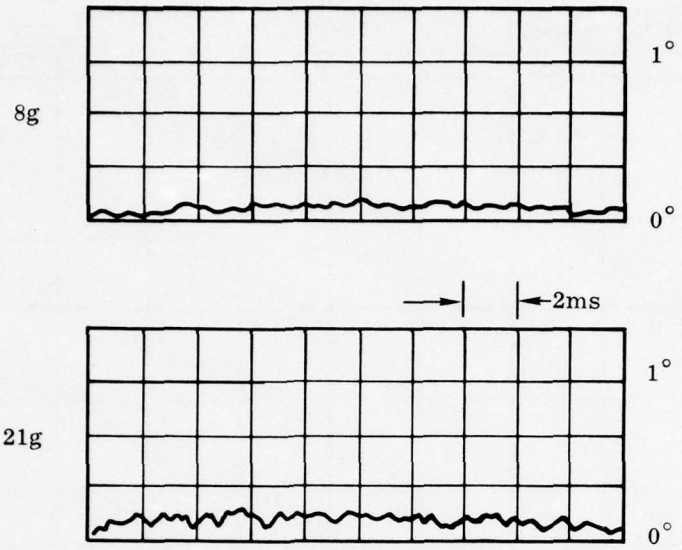

INSERTION LOSS

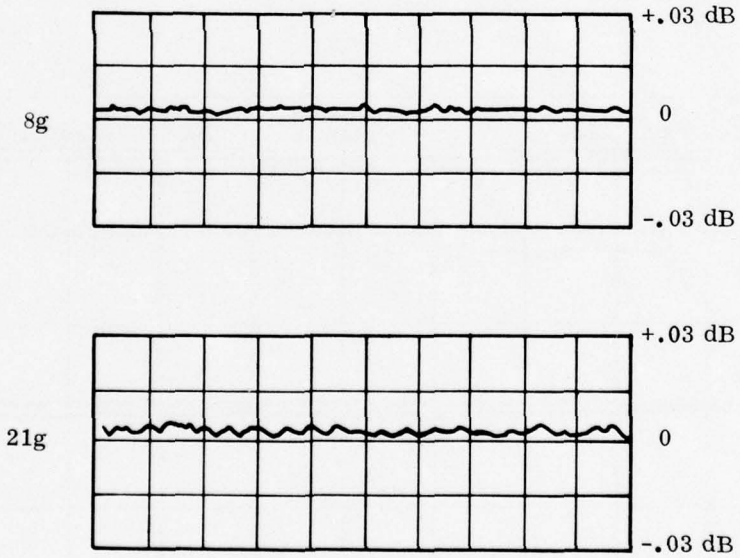

The Above Tests Were Measured on Port #2 of the Interconnect Module, While Being Vibrated in the Longitudinal Axis.

Figure 25. Oscilloscope Presentations of Phase and Amplitude Variations During Vibration

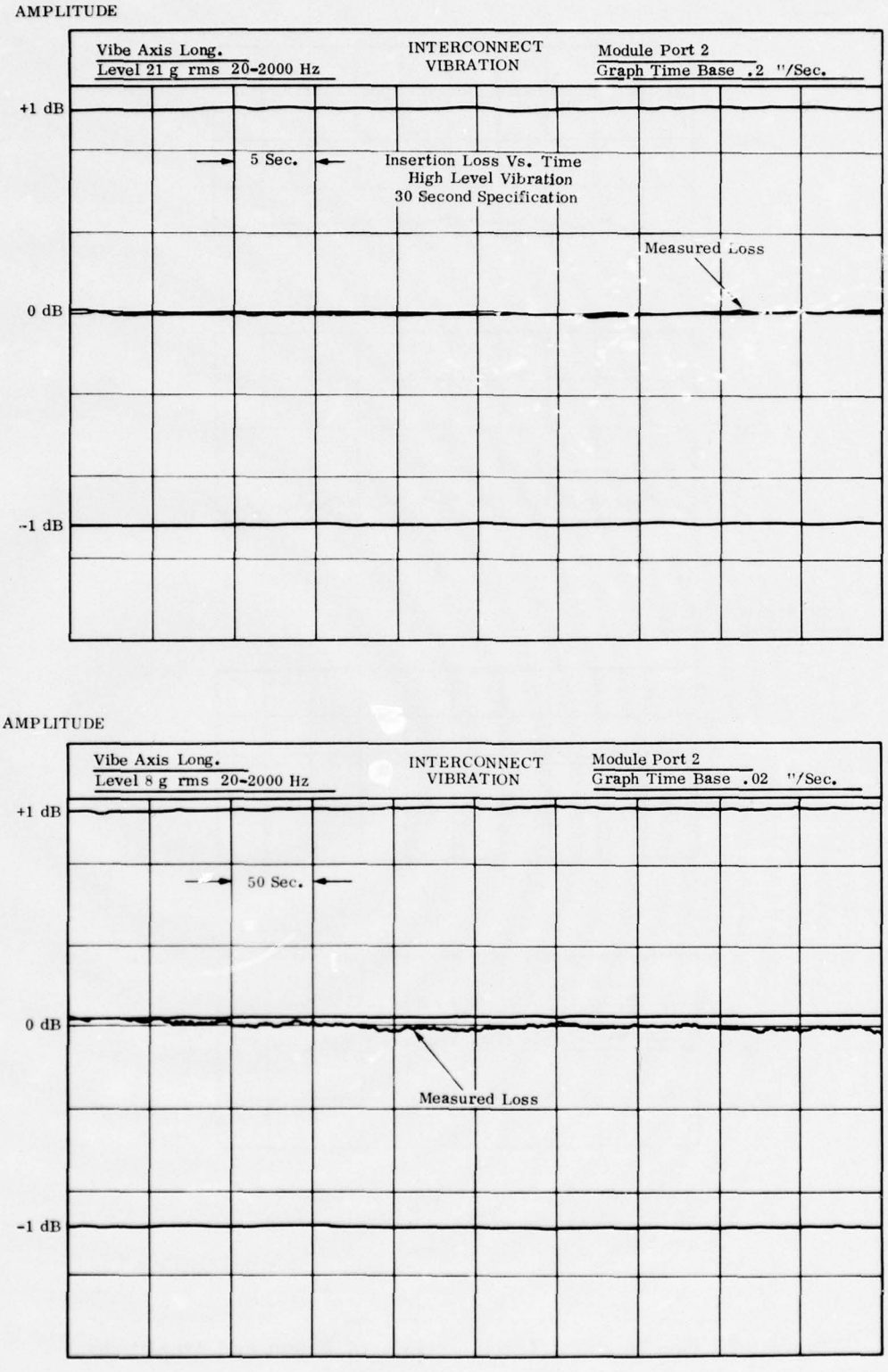

Figure 26. Long Term Insertion Loss Changes During Vibration

3.2.2.5 Leakage Performance. Good microwave connectors prevent undesired coupling of module microwave signals by maintaining a low value of leakage signal. The leakage signal performance of the interconnect design illustrated in Figures 13, 14, and 15 was measured using the test setup shown in Figure 27. Test results show that these connectors passed the leakage requirement given in Table 1, requirement 6 (-90 dB maximum), before the design value of fastening screw torque was reached.

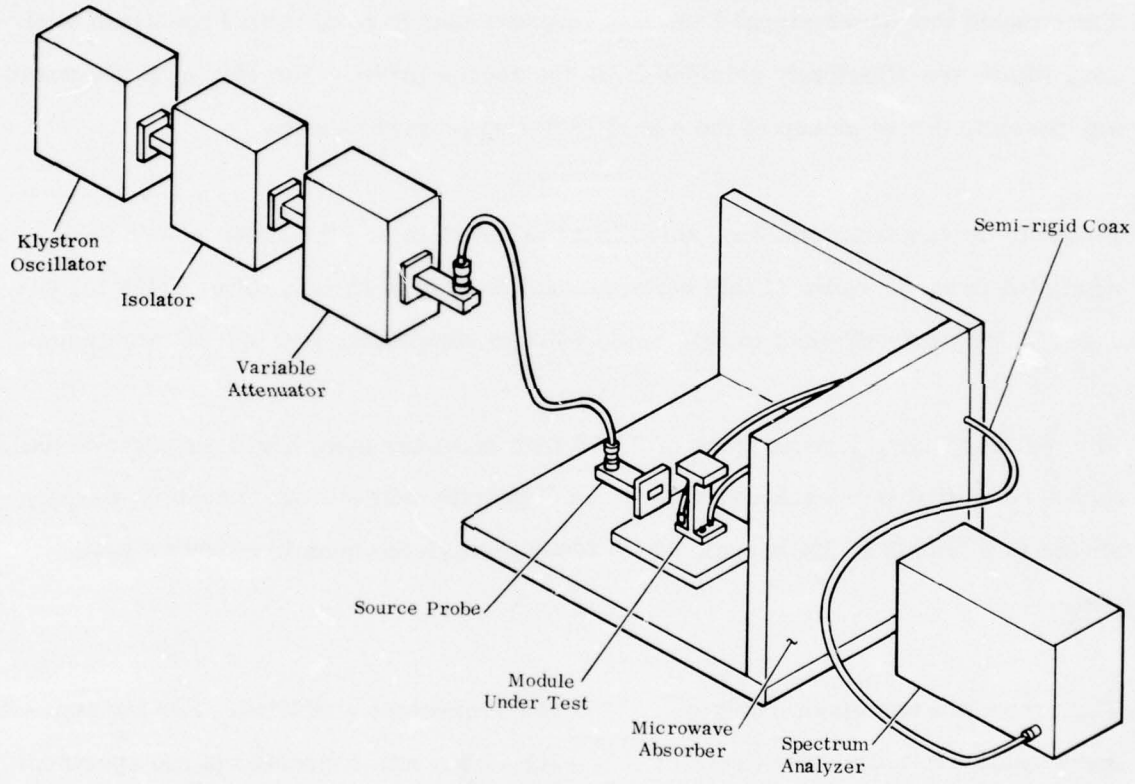

Figure 27. Module Interconnection Leakage Test Setup

The leakage test was conducted by radiating a high level microwave signal in the vicinity of the connector under test and measuring the power level induced into the cable leading from the connector.

Figure 27 illustrates the method of generating the high level (+20 dBm) Ku band signal. The isolator prevents undesired reflected signals from reaching the klystron oscillator. The variable attenuator allows the source power to be adjusted to +20 dBm, using a power meter. A coax-to-waveguide transition was used as a source antenna probe. A length of coax cable provided for worst case positioning of the source probe in the vicinity of the connector under test.

The coupled low power signal level was measured using a calibrated spectrum analyzer, which was effectively shielded from the source probe. The shielding prevented any possible direct pickup of the signal radiating from the probe.

Because the spectrum analyzer noise level is -90 dBm and the probe power is +20 dBm, the dynamic range of this measurement is limited to -110 dBm. This is, however, more than sufficient to determine leakage compliance to a -90 dB requirement.

For test purposes, a short piece of 0.085 inch diameter semi-rigid coax was installed on the module side of each connector. The opposite side of each connector was connected to a female OSSM barrel, which feeds through the module mounting base plate.

The procedure used tested only one of the two connectors at a time. For the connector under test, the 0.085 inch diameter semi-rigid coax was connected to the spectrum analyzer and the corresponding OSSM barrel was terminated in a 50 ohm load. The 0.085 inch diameter semi-rigid coax not under test was left open circuited.

The leakage level was measured with respect to fastening screw torque for each connector and for three different matings of each connector. Figure 28 provides a plot of the measured data, with reference lines showing leakage and torque requirements, and limit of measurement capability. Each line represents a different mating of the connector and the performance achieved, starting at 8 inch-ounces of torque and

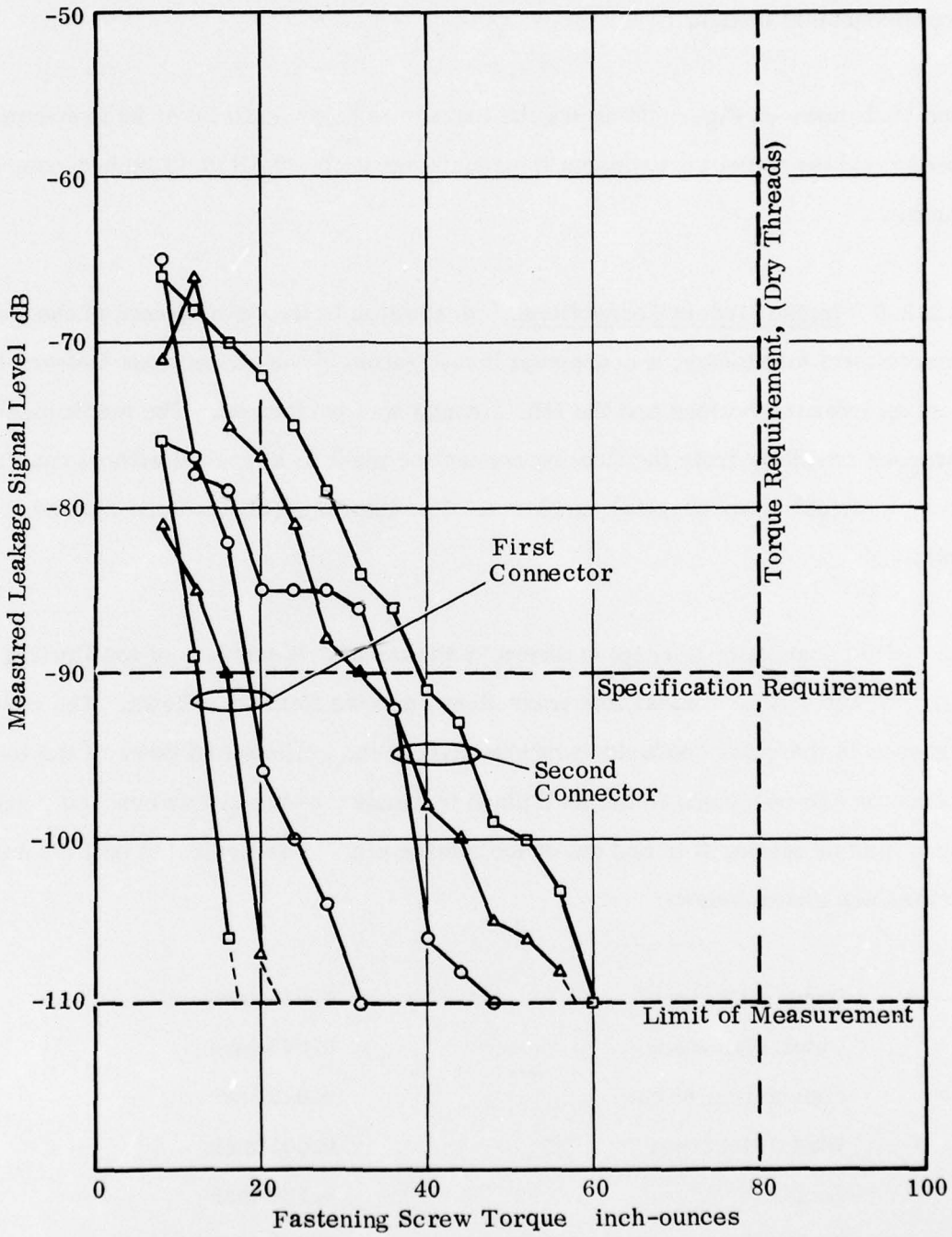

Figure 28. Measured Leakage Level vs Fastening Screw Torque

increasing in steps of 4 inch-ounces to 60 inch-ounces of torque. Torque of 80 inch-ounces for dry threads is proposed as a design objective consistant with screw size and mechanical design.

The best curve of Figure 28 shows the leakage is below -110 dB at 20 inch-ounces of torque and the worst curve meets the requirement of -90 dB at 40 inch-ounces of torque.

3.2.2.6 Inside Module Connections. In addition to the development of the module interconnect technology, a conceptual investigation of the connections between the floating interconnections and the MIC circuits was performed. The mechanical stresses resulting from the floating connection must be absorbed without causing serious electrical or mechanical problems. Two interconnections were studied in some detail.

An in-line connection concept is shown in Figure 29. It consists of the floating interconnect, the MIC to coaxial line transitions, and the flexible bellows. The resulting stresses in the outer conductor are absorbed in the bellows and those of the inner conductor are overcome in the X-Y plane by bending of the center conductor and in the Z axis by sliding it in and out of the mating pin. The desirable bellows parameters are shown below:

Inner diameter:	0.046 inch
Outer diameter:	0.073 inch
Convolution pitch:	0.010 inch
Wall Thickness:	0.001 inch
Length:	0.100 inch
Spring Rate per Convolution:	100 lbs./inch
Maximum deflection:	±0.025 inch

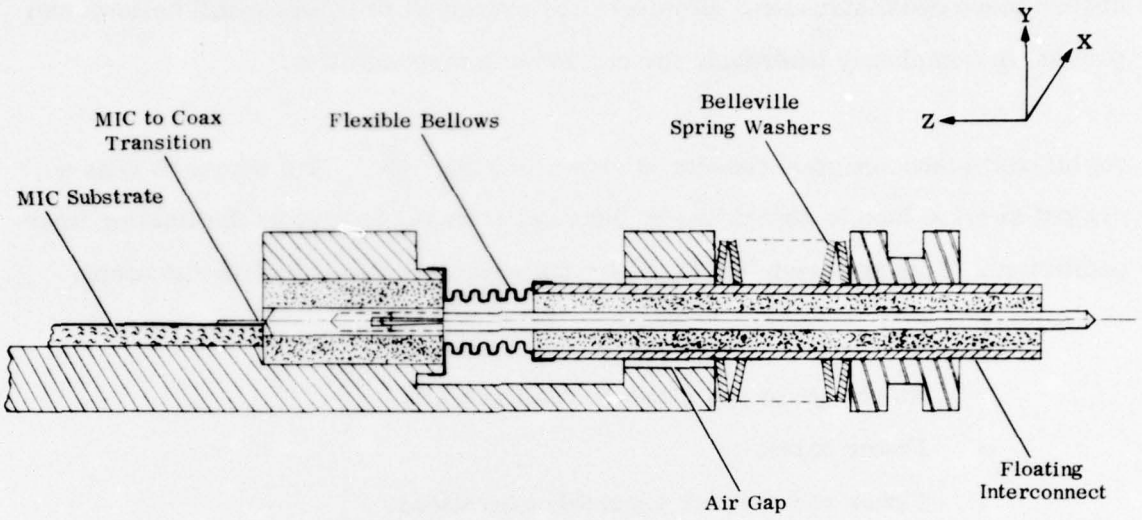

Figure 29. In-Line Connection Concept

These parameters result in a 50 ohm transmission line. The VSWR effect caused by the convolutions of the bellows was determined analytically. Using the impedance transformation approach it is easy to determine the amount of reactance contributed by each convolution which in this case is $jX/Z_o = j0.007$. Using a total of 10 convolutions results in a normalized impedance of $\frac{Z}{Z_o} = 1.0 - j0.07$. This corresponds to a VSWR of 1.073:1 which in turn causes a fixed phase shift of about 2°.

Another possible source for a mismatch and phase problem is due to eccentricity of the center conductor with respect to the outer conductor. It was found that this can only occur if the critical buckling pressure of the bellows is exceeded.

The described concept will not leak RF energy since both ends of the bellows are soldered.

An attempt was made to use the bellows for the dual function of providing the necessary contact pressure for the floating interconnect, as well as the flexible interconnect to absorb mechanical stresses. However, the maximum pressure small bellows can provide is completely inadequate for a reliable interconnection.

An off-set interconnection concept is shown in Figure 30. This approach uses a coaxial service loop to absorb the mechanical stresses caused by the floating interconnection. This approach has the following advantages over the first concept:

- No change in VSWR due to radii changes.
- No change in phase due to radii changes.
- Fewer parts.
- Fewer and simpler assembly operations.

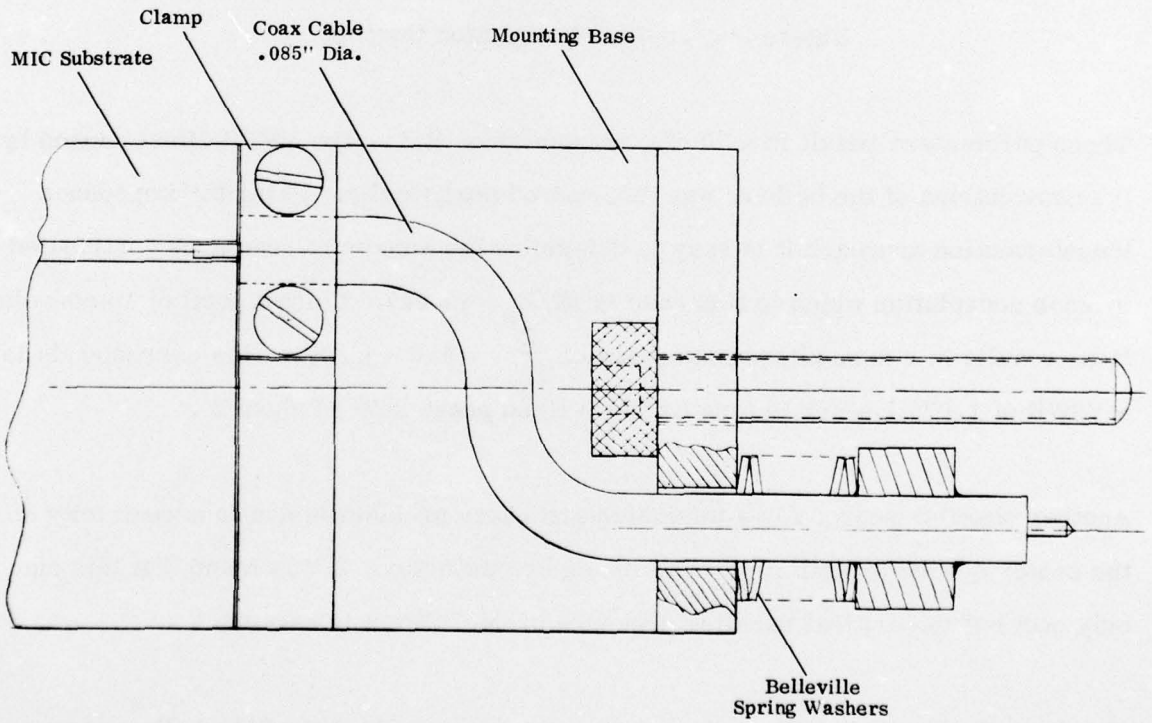

Figure 30. Inside Module Connection Concept with Bendable Coaxial Cable

The disadvantages are:

- More space is required.
- The module length is slightly greater.
- The RF sealing at the MIC-coaxial clamp is not as good due to the finite gap in the clamp.

In summary it can be stated that both interconnecting concepts are practical. The choice depends upon the actual application.

3.2.2.7 Production Cost Analysis of Phased Array Module RF Interconnection Technique. In any comprehensive cost analysis or design to cost synthesis, several factors must be applied. The keynote is simplicity of design and ease of fabrication. The goal is to reduce the total fabrication time and design for the simplest manufacturing method based on quantity. Generally, it is more economical to make large integrated parts of single piece design than parts consisting of several joined pieces.

Even though minor design modifications may be made prior to the final interconnect design freeze, the basic RF interconnect technique developed during this program embodies many of the design to cost criterias.

Simplicity is maintained through the use of the minimum number of parts to accomplish the task at hand.

A single 0.125 inch diameter dowel pin, performs as an alignment tool protecting the exposed male connector pins during assembly as well as insuring good connected strength so important during environmental stress.

The coaxial connectors are the subminiature series manufactured by Omni Spectra, Inc. of Farmington, Michigan. These connectors have proven ruggedness and reliability as well as low VSWR. The semi-rigid cable center conductor is used as the

connector center contact pin and thus an additional part is eliminated. On the distribution manifold side of the interconnect, a standard stripline compatible receptacle will be used.

In an assembly as complicated as an active antenna module which must be combined in an array structure with 31 identical modules and electrically connected to a multiple function microwave power distribution manifold, several joined pieces are required. The requirement stems particularly from the need to tune each of the antenna apertures to reduce mutual coupling.

Three alternatives presently exist for tuning the apertures of the phased array modules, depending upon the final design and test restraints.

a. No individual tuning in the module. The aperture is machined or casted and then tested, possibly in an automated manner. If the test is passed, the aperture is assembled into the transmitter/receiver module interconnecting with the module through a waveguide interface.

b. Individual tuning in the module. After manufacture similar to a, the aperture is assembled into the next stage of the module, the duplexer, which consists of a 4 port circulator. A tuning element is then adjusted for minimum return power in the receiver leg of the duplexer while the transmitter leg is excited over the required bandwidth. The antenna/duplexer is then assembled into the remainder of the module through either a coaxial interface or microcircuit, microstrip bridge.

c. Individual tuning of all modules simultaneously in an array structure with the modules phased to a predetermined pointing angle. After manufacture and assembly with the 4 port circulator similar to b, the entire array of 32 modules are assembled and driven from a 32 element power distribution network.

The array is then statically steered to a predetermined pointing angle in space, and the module tuning elements are then adjusted for minimum return powers on the receiver legs of each the duplexers. This would probably be an interactive process. After tuning, the individual antenna/duplexers would be assembled into the final module configuration through either a coaxial interface or microstrip bridge.

The problem is antenna mutual coupling. In the proposed 32 element array, the array is small enough such that each module antenna is inserted into a different environment depending upon its position inside the array. This variation may present a requirement for individually tuning each module in the array.

A fully modular concept, with interchangeable modules of identical function, requires commonality of design and would dictate the reduction of the interelement mutual coupling through applied design techniques such as increased spacing or some type of radiation suppressor between modules. If these techniques do not produce acceptable results, one of the individual fine tuning requirements will necessarily exist.

The module interconnection requirements are dictated by the individual module tuning requirements.

Ease of testing would necessitate a connector at each point where test equipment must be connected.

Under the worst situation where the module must be tested at various levels of assembly, several interconnects must be used. For this reason, the cost of the coaxial RF interconnection developed during this program is even more important.

SECTION 4

TECHNOLOGICAL FORECAST

4.1 PROBLEM NO. 1

Microwave radio frequency interconnects applicable to an X-band, $\lambda/2$ spaced, modular phased array were not available. Military specifications also are not known to exist for this requirement. The specific requirements of amplitude and phase tracking between an array grouping of interconnects is uniquely applicable to the nongimballed, electronically scanned, phased array and more specifically applicable to an antenna array which may be used in an accurate and linear angle tracker. Linearity is required by a missile target seeker of the active or semi-active variety. The nonavailability of this type of specialized connector imposed a potential cost impact on a modular phased array which may require in excess of 100 microwave interconnections.

4.1.1 Potential Benefits

Solution of this problem, as generally stated, will provide one of the necessary technological bases required for the realization of an airborne electronically steered phased array radar. Especially a radar which is practical, from the standpoints of cost, accuracy, reliability and maintainability.

4.1.2 Solution

The solution which was developed is applicable to other single and multifunction airborne electronic systems, plug-in radio frequency/microwave modules other than antenna modules, as well as many modular radio frequency/microwave commercial applications.

The significant aspects of the interconnect are:

- A small interface area used for two connectors (less than 0.35 square inches).
- Less than 2 electrical degrees of differential phase variation from -65 to +110°C at 13.3 GHz.
- Less than 3 electrical degrees of phase variation through 500 connections.
- Excellent vibration and shock stress immunity.
- Use of standard parts and materials.
- Less than 0.08 dB insertion loss variation through 500 connections.

4.1.3 Suggestions and Implications

Because of the many potential uses, the microwave interconnect technology developed during this program should be expanded into hardware requirements and specifications. Final engineering should be accomplished on the specific solutions produced by this program as well as alternative configurations which may evolve from them.

4.2 PROBLEM NO. 2

The spectral noise characteristics of an injection locked IMPATT oscillator were not known. The amount of AM and FM noise transmitted in a doppler radar is critical to system operation in the presence of clutter return.

Gaining this knowledge provided another of the technological bases required for the realization of an active, airborne, electronically steered, phased array radar.

4.2.1 Measurements

AM and FM noise was measured in a 1 kHz bandwidth for two IMPATT transmitters, over a temperature range from -55 to +70°C and versus injection gains of +16 dB, +11 dB and +6 dB. Vibration susceptibility was also measured.

Analysis indicated that both IMPATT amplifiers tested had adequate spectral noise performance over both temperature and vibration ranges when operated at an injection gain of +11 dB, and in an array totaling 250 watts of transmitted power.

SECTION 5

ACKNOWLEDGEMENTS

The following personnel of the Teledyne Ryan Electronics Engineering Department made contributions to the reported development program:

H. Penner, Project Engineer

H. Otzen, Microwave Group

B. Kipp, Microwave Group

G. Murdock, Systems Analyst

R. Mayberry, Microwave Group

D. Longacre, Systems Engineering

K. Roberts, Antenna Design

The Government's Technical Engineering Representative for this program was Mr. S.A. Barham, Naval Sea Systems Command, Code SEA 0341.

APPENDIX A

Change in effective short position, due to semi-rigid cable expansion:

Longitudinal cable length is function of copper jacket

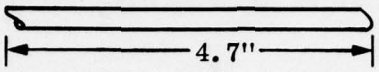

$= \ell_o$

$$\Delta\phi_c = \left(\frac{\ell - \ell_o}{\lambda_d}\right) \quad (360)$$

$$\ell = \ell_o (1 + \delta_{cu} \Delta T)$$

$$\Delta T = T - T_o$$

$$\lambda_d = \frac{\lambda_o}{\sqrt{\epsilon}}$$

$$\Delta\phi_c = \frac{360 \sqrt{\epsilon_o}\, \ell_o\, \delta_{cu}\, \Delta T}{\lambda_o}$$

$\epsilon = 2.1$

$\ell_o = 4.7"$

$\delta_{cu} = 1.61 \times 10^{-5}/℃$

$\lambda_o = .8874"$

$T_o = 22℃$

T	$\Delta\phi_c$
-65℃	-3.87°
-60℃	-3.65°
-40℃	-2.76°
-20℃	-1.87°
0℃	-.98°
40℃	.76°

T	$\Delta\phi_c$
60℃	1.69°
80℃	2.58°
100℃	3.47°
120℃	4.36°
140℃	5.25°
150℃	5.69°

2. Change in effective short position, due to contraction of Teflon dielectric:

Cable's dielectric shrinks at temperature below fabrication temperature (22°C). Gap in dielectric results in different velocity of propagation.

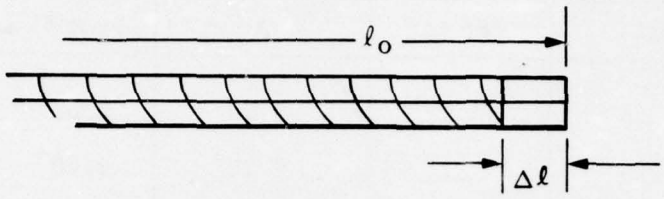

$$\Delta\phi_T = \frac{\Delta\ell}{\lambda_o} \times 360 - \frac{\Delta\ell}{\lambda_d} \times 360 = \frac{\Delta\ell\, 360}{\lambda_o} (1 - \sqrt{\epsilon})$$

$$\Delta\ell = \ell_o (1 + \delta_{cu} \Delta T) - \ell_o (1 + \delta_{TEF} \Delta T)$$

$$= \ell_o \Delta T (\delta_{cu} - \delta_{TEF})$$

$$\therefore \phi_T = 360\, \ell_o \Delta T (\delta_{cu} - \delta_{TEF}) \frac{1 - \sqrt{\epsilon}}{\lambda_o}$$

ℓ_o = 4.7"
δ_{cu} = 1.61×10^{-5}/°C
δ_{TEF} = 9×10^{-5}/°C
ϵ = 2.1
λ_o = .8874"
$\Delta T = T - T_o$
T_o = 22°C

T	$\Delta\phi_T$
-65°C	-5.51°
-60°C	-5.19°
-40°C	-3.92°
-20°C	-2.66°
0°C	-1.39°

Not Valid >22°C

3. Correction to measured data is sum of $\Delta\phi_c$ and $\Delta\phi_T$.

Temp	Measured Phase		Correction	Corrected Values	
	Port #1	Port #2	$\Delta\phi_c + \Delta\phi_T$	Port #1	Port #2
-65°C	-6.33°	-6.15°	-9.38°	3.05°	3.23°
-45.6°C	-5.29°	-5.29°	-7.29°	2.00°	2.00°
-17.8°C	-4.26°	-4.62°	-4.29°	0.03°	-0.33°
+10°C	-2.43°	-2.45°	-1.30°	-1.13°	-1.15°
+22°C	0°	0°	0°	0°	0°
+37.8°C	.63°	.69°	.70°	-.07°	-.01°
+65.6°C	1.60°	1.88°	1.94°	-.34°	-.06°
+93.3°C	1.53°	2.32°	3.17°	-1.64°	-.85°
+121.1°C	.87°	2.64°	4.41°	-3.54°	-1.77°
+150°C	2.14°	4.79°	5.69°	-3.55°	-.90°

Corrected values, and differentials are plotted in graph (Figure 18).